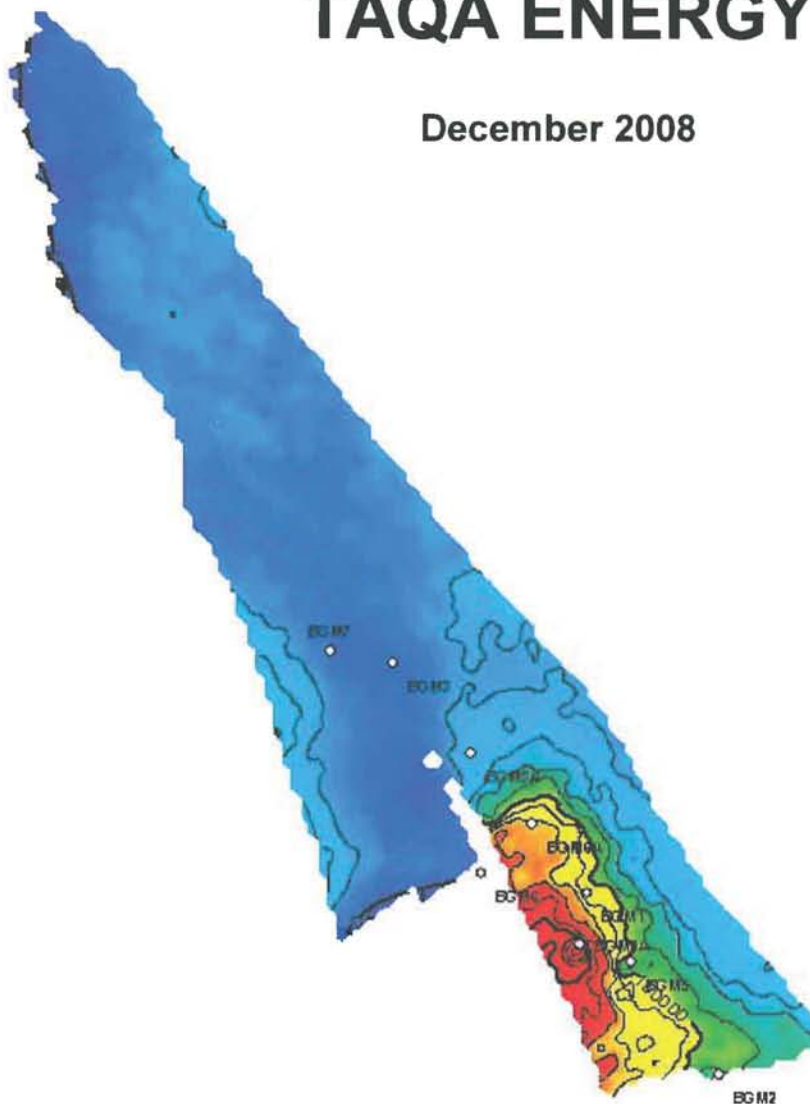


# **BERGERMEER UGS MODELING STUDY, PHASE 4**

## **TAQA ENERGY**

**December 2008**







# BERGERMEER UGS MODELING STUDY, PHASE 4

23 December 2008

PREPARED FOR **Taqa Energy B.V.**

Prinses Margrietplantsoen 40  
P.O.Box 11550  
2502 AN The Hague  
The Netherlands

BY **SGS Horizon bv**

Prinses Margrietplantsoen 81  
2595 BR The Hague  
The Netherlands

	NAME	SIGNED	DATE
PREPARED BY	Jeroen Mullink		
	Hans Martens		
APPROVED BY	Abu Faithfull		

SGS Horizon bv has made every effort to ensure that the interpretations, conclusions and recommendations presented herein are accurate and reliable in accordance with good industry practice and our quality management procedures. SGS Horizon bv does not however guarantee the correctness of any such interpretation and shall not be held liable or responsible for any loss, costs damages or expenses incurred or sustained by any resulting from any interpretation or recommendation made by any of our officers, agents or representatives.



# Table of Contents

<b>LIST OF TABLES .....</b>	<b>3</b>
<b>LIST OF FIGURES .....</b>	<b>5</b>
<b>EXECUTIVE SUMMARY .....</b>	<b>13</b>
<b>1 INTRODUCTION .....</b>	<b>14</b>
<b>2 GEOLOGICAL MODEL ADJUSTMENTS .....</b>	<b>16</b>
2.1 PHASE 4 OBJECTIVES .....	16
2.2 ALTERNATE TOP STRUCTURES.....	16
2.3 VERTICAL RESERVOIR QUALITY DISTRIBUTION .....	20
2.4 UPSCALING / GRID DIMENSIONS .....	26
<b>3 WELL TEST MODELING.....</b>	<b>28</b>
3.1 INTRODUCTION .....	28
3.2 CORE PERMEABILITY AVERAGES.....	28
3.3 RESERVOIR HEIGHT AS SEEN BY WELL TESTS.....	29
3.4 WELL TEST MODELING WITH ECLIPSE DYNAMIC MODEL.....	31
3.5 BGM-1 WELL TEST MODELING RESULTS.....	32
3.5.1 BGM-1 well test 1986.....	32
3.5.2 BGM-1 well test 1987.....	33
3.5.3 BGM-1 well test 1997.....	35
3.6 BGM-7 WELL TEST MODELING RESULTS.....	36
3.6.1 BGM-7 well test 1994.....	37
3.6.2 BGM-7 well test 1997.....	38
3.7 CONCLUSION.....	39
<b>4 HISTORY MATCH.....</b>	<b>43</b>
4.1 PHASE 4 MODEL CHANGES .....	43
4.2 REALIZATIONS .....	43
4.3 HISTORY MATCH RESULTS.....	44
4.4 AQUIFER SENSITIVITIES.....	51
4.5 GWC BEHAVIOUR.....	59
4.6 CONCLUSIONS .....	62
<b>5 UGS DEVELOPMENT SCENARIOS .....</b>	<b>63</b>
5.1 UGS INPUT DATA.....	63
5.1.1 UGS subsurface realizations.....	63
5.1.2 UGS offtake scenario .....	63

5.1.3	<i>Cushion / working gas injection scheme</i> .....	64
5.1.4	<i>UGS well parameters</i> .....	65
5.2	UGS MODELING RESULTS PHASE 4 .....	66
5.2.1	<i>UGS characteristics</i> .....	66
5.2.2	<i>UGS GWC behaviour</i> .....	70
5.3	WELL TRAJECTORY PLANNING .....	71
5.4	WELL PRODUCTIVITY ESTIMATES FROM STATIC MODEL .....	79
5.5	HYSTERESIS AND NON-TANK BEHAVIOR .....	82
5.6	UGS CAPACITY CURVES .....	92
5.7	WATER DISPOSAL BGM-3A .....	92
<b>6</b>	<b>CONCLUSIONS AND RECOMMENDATIONS</b> .....	<b>95</b>
	<b>REFERENCES</b> .....	<b>97</b>
<b>7</b>	<b>APPENDIX I</b> .....	<b>98</b>
7.1	WELLTEST MODELING STATISTICS .....	98
7.2	UGS PERFORMANCE CURVE PARAMETERS .....	100
<b>8</b>	<b>APPENDIX II : PVT-STUDY (PHASE 3)</b> .....	<b>103</b>
8.1	COMPOSITION DEFINITION ORIGINAL BERGERMEER GAS .....	103

## List of Tables

Table 3-1	BGM-1 average core permeability, geometric mean, 90% scaled. ....	28
Table 3-2	BGM-1 well test interpretation results using Sapphire. ....	30
Table 3-3	Well test-KH from latest test in existing BGM-wells, taken from Phase2 report Table 2-5 and Table2-6. The value for BGM-7 is the drawdown-KH (BU-KH is 330 mDm). (*) was previously interpreted by TAQA. ....	30
Table 3-4	Comparison of KH values as found by PTA-analysis of the build-up period (with Kappa, see phase 2), by well test modeling with Eclipse100 and as found for the existing BGM wells in the phase4 models. For BGM-7 the KH of the drawdowns is compared. The KH in the models is taken from the perforated sections at the time of the test. The (*) behind some of the wells indicates that the KH values for PTA analysis come from interpretation done by TAQA. ....	41
Table 3-5	As Table 3-4, but now KH values from PTA and WTM compared with total reservoir KH in the phase4 models. ....	42
Table 4-1	GIIP and reservoir pressure at beginning and end of history match, phase 4 models. The summer injection test of 2007 and 2008 production is included. The initial reservoir pressure is 227.8 bara at 2100 m tvdss. ....	43
Table 4-2	Phase 4 realisations. ....	44
Table 4-3	Phase 4 History Match Parameters per realization. ....	45
Table 4-4	Realisations table for runs including the aquifer, INTERB and UBELL sensitivities. ....	52
Table 4-5	Overview of HM quality using pressure and GWC points at certain moments in time. For reference, the base case from phase 2 (DISMIDHIGHKV_BELL050 is also given. ....	62
Table 5-1	Main phase 4 subsurface realizations. ....	63
Table 5-2	Possible offtake scenario's from Phase 2 with Phase 4 base case. ....	63
Table 5-3	UGS parameters Phase 4 base case (INTERA_DISMID_ALT2_BELL050), no aquifer. ....	64
Table 5-4	Summary of UGS modeling results of the 88/133 UGS scenario. End-prod rest dP is the pressure loss in the 8 days between end of production and start of injection. End-inj dP likewise after injection. The pressures are taken from the gridblocks around the wellbores and are thus different from the average reservoir pressure, see also Figure 5-1. ....	66
Table 5-5	Cushion and working gas volumes for alternate pressure scenario (133 – 77 bar), base case subsurface model (INTERA_ALT2_BELL050). ....	69
Table 5-6	Summary of aquifer sensitivities UGS modeling. ....	69
Table 5-7	Static trend based estimates for the HPROP KH's in the 'InterA' top structure. ....	81
Table 5-8	Well performance parameters for base case model BGM_INTERA_DISMID_ALT2_BELL050_UGS_TESTS. ....	92

Table 7-1	Statistics welltest modeling BGM-1 1986.....	98
Table 7-2	Statistics welltest modeling BGM-1 1997.....	98
Table 7-3	Statistics welltest modeling BGM-7 1994.....	98
Table 7-4	Statistics welltest modeling BGM-7 1997.....	98
Table 7-5	Statistics welltest modeling BGM-1 1987.....	99
Table 7-6	Well performance curve parameters base case 'INTERA_BELL050'.....	100
Table 7-7	Well performance curve parameters low vertical well productivity case 'INTERB_BELL033'.....	100
Table 7-8	Well performance curve parameters high productivity case 'INTERA_BELL080'.....	100
Table 7-9	Well performance curve parameters base case productivity with aquifer 'INTERA_BELL050_LOWCUSHION'.....	101
Table 7-10	Well performance curve parameters low horizontal well productivity 'HIGHP'.....	101
Table 7-11	Well performance curve parameters low vertical productivity case 'INTERB_BELL033', with lower skins, see Table 7-13.....	101
Table 7-12	Well performance curve parameters low vertical productivity case 'INTERB_BELL033', with lower skins, see Table 7-13.....	102
Table 7-13	Darcy and non-Darcy skin values for LOWSKIN sensitivity runs for performance parameters.....	102



## List of Figures

Figure 1-1	Location of the Bergermeer field in the Bergen concession, projected on a KH-map [mDm] of the Bergermeer reservoir above the GWC-contact. The main UGS is in the southeast of the field, where also most of the production-wells are located.....	15
Figure 2-1	Uncertainty map for Top ROSLU. Uncertainty is expressed in m, top ROSLU well picks are plotted as red squares.....	18
Figure 2-2	'InterA' uncertainty proportion trend map, ranging from multiplier 1.0 in the north to 0.0 in the south. For reference the top ROSLU well picks are plotted as well (cf. Figure 2-1).....	19
Figure 2-3	'InterA' (left) and 'InterB' (right) uplifts w.r.t. base structure maps. Offset is in m, red squares mark top ROSLU well picks. The maps are smoother than the input uncertainty map as a result of the Petrel gridding process [1]. .....	19
Figure 2-4	NS section of the field, just East of BGM1, viewed from the East. The yellow line indicates the base top structure according to seismic interpretation, the white line the original GWC. The cross-section highlights some extrapolation issues towards the eastern boundary fault (in the H case vs. the others). These are caused by the fact that the Petrel mapping & well correction are not 100% controllable; nevertheless overall fractions are honored. ....	20
Figure 2-5	BGM1 core permeabilities (Klinkenberg-corrected) vs. distance from top reservoir. The data exhibits a steep exponential trend with a porosity increase of about 8.6 % per m from top ROSLU downwards. ....	21
Figure 2-6	Correlation panel for the PHIE log from BGM1 to BGM8 (L to R). The wells are aligned at the top ROSLU, the depth scale at the left is from BGM1. The deterioration of the reservoir quality towards the top is universal, but there are quantitatively significant differences in the degree of deterioration. ....	22
Figure 2-7	Overlay of the PHIE logs of BGM1 (line) to BGM7 (colours). The wells are aligned at the top ROSLU, depth scale is from BGM1. Both wells show a deterioration of the reservoir quality to the top, but at relevant depths BGM7 is several (4) PU's better, which maps to significantly higher permeabilities for the poroperm used (factor 5). ....	22
Figure 2-8	Bell multiplier profile plotted along the BGM1 track. Top reservoir is indicated, as is the GR and PHIE log, as well as the (final) perforation status. The 'BELL050' curve has, in combination with an overall multiplier from matching to well test KH's (chapter 3), the value 0.5 in the centre, 0.15 at the top. ....	23
Figure 2-9	Plot of BGM1 Klinkenberg-corrected core permeability vs. k-layer index in the static model (which has 150 layers). The core permeabilities are binned by groups of 10 k layers; the P50 of each bin is also plotted.....	23

Figure 2-10	Permeability in dynamic model cells that have (PHIE) log values as their base (i.e. where the fine static model has 'upscaled cells'). No multiplier has been applied, apart from the 'khkv' correction (see above). The binned core values from Figure 2-9 are plotted, along with similar binned values of the upscaled cell data. ....	24
Figure 2-11	Permeability in the 'BELL050' dynamic model vs. static model K index. The 'BELL050' multiplier includes well-test based correction (Figure 2-8). The binned core values from Figure 2-9 are plotted, along with similar binned values of the cell data. The profile is more conservative than core & well data (Figure 2-9, Figure 2-10), except for the top 15 m of the reservoir (the top 10 fine K layers). Note the vertical alignment of the points indicating the finer simulation grid at the top (section 2.4).....	25
Figure 2-12	Permeability in the 'HIGHP' dynamic model vs. static model K index. The 'HIGHP' permeability includes a well-test based correction (Figure 2-8). The binned core values from Figure 2-9 are plotted, along with similar binned values of the cell data. The profile is more conservative than core & well data (Figure 2-9, Figure 2-10), as a consequence of well test matching, and honours the core trend in the top 15 m of the reservoir (the top 10 fine K layers). Moreover, the scatter around the trend is less. The 'HIGHP'-porosity also deteriorates more steeply towards the top. Note the vertical alignment of the points indicating the finer simulation grid in the upper reservoir section (see section 2.4). ....	26
Figure 2-13	View of porosity in upscaled grid with BGM-7 (left) and BGM-6A (right).....	27
Figure 3-1	BGM-1 core permeability vs. Phase 2 model permeability. Model average permeability is upscaled in Petrel using the diagonal tensor method (harm/arithm.) Note that the best section has no core coverage due to the unconsolidated nature of the section.....	29
Figure 3-2	Radial LGR of BGM-1, with NR=20, Theta=4, top view (left) and cross-section of 3D permeability model with range 0 – 2500 mD (right).....	31
Figure 3-3	Match of BGM-1 well test from 1986 with phase2 base case UGS model, rate (left) and pressure (right) vs. time (hours).....	33
Figure 3-4	Match of BGM-1 well test from 1986 with phase2 base case UGS model, log-log-plot.....	33
Figure 3-5	Match of BGM-1 well test from 1987 with base case UGS model, rate (left) and pressure (right) vs. time (hours).....	34
Figure 3-6	Match of BGM-1 well test from 1987 with base case UGS model, log-log-plot.....	35
Figure 3-7	Match of BGM-1 well test from 1997 with phase2 base case UGS model, rate (left) and pressure (right) vs. time (hours).....	36
Figure 3-8	Match of BGM-1 well test from 1997 with phase2 base case UGS model, log-log-plot.....	36
Figure 3-9	PTA-analysis of the 1994 well test in BGM-7. Log-log plot of the BU's (left) and DD's (right). The KH from the BU's is 200-277 mDm, from the DD's a KH is calculated of 700 to over 2000 mDm for DD#1, resp. DD#3. ....	37

Figure 3-10	Match of BGM-7 well test from 1994 with phase2 base case UGS model, left BU-match, right DD-match. ....	38
Figure 3-11	Match of BGM-7 well test from 1994 with phase 2 base case UGS model, log-log-plot of BU#3 with horizontal barriers below perfs (left) and without Kz=0 below perfs (right). ....	38
Figure 3-12	Match of BGM-7 well test from 1997 with phase 2 base case UGS model, rate (left) and pressure (right) vs. time (hours). Note that while BU#1 matches well, the drawdowns are much too large. ....	39
Figure 3-13	Match of BGM-7 well test from 1997 with phase 2 base case UGS model, log-log-plot. The near wellbore region did not match perfectly, the KH is approximately correct. ....	39
Figure 3-14	Comparison of KH values as found by PTA-analysis, well test modeling with Eclipse100 and as found for all existing BGM wells in the Phase4 models (Table 3-4). The line plotted is $y=x$ . ....	41
Figure 3-15	Comparison of well test-KH with total KH available in the various dynamic models of phase4. The dynamic model KH's are over the full top→GWC range. For comparison, the KH computed over the static model, without upscaling or multiplier (BELL or otherwise) is also shown ('Fine'). For the BELL033 and BELL080 models, the KH-values are 2/3 and 8/5 of BELL050. Note that both well BGM3A and BGM6A are not used in property modeling [1], hence there is more scatter between the dynamic models for these wells. ....	42
Figure 4-1	Effect of LGR on water coning behaviour. The LGR is in the picture on the left. Without LGR (right), the cone is overestimated. ....	45
Figure 4-2	HM comparison of WBHP in the base case (red), BC with LGR (blue) and BC with LGR and BELL multiplier (green). In the base case, without LGR, the water production is overestimated, BHP is 0 bar as water breaks through. The effect of the BELL-multiplier is stronger than the LGR as in this case water breakthrough is earlier than in the base case. ....	46
Figure 4-3	Location of baffles in HIGHP-scenario, visualised by 3D model of transmissibilities. Red is the gas-leg, green is the water-leg. The baffle-transmissibility is ca 10* that in the main fault. ....	47
Figure 4-4	Pressure match base case (INTERA_BELL050), P/Z curve (left) and deflection from straight line (right) for BGM-1, BGM-3A and BGM-7. ....	47
Figure 4-5	GWC-match base case (INTERA_BELL050) of BGM-1 and BGM-7 (left) and water-production BGM-7 (right). ....	48
Figure 4-6	Pressure match base case (INTERB_BELL050), P/Z curve (left) and deflection from straight line (right) BGM-1, BGM-3A and BGM-7. ....	48
Figure 4-7	GWC-match base case (INTERB_BELL050) of BGM-1 and BGM-7 (left) and water-production BGM-7 (right). ....	48
Figure 4-8	Pressure match low case horizontal productivity (HIGHP), P/Z curve (left) and deflection from straight line (right) BGM-1, BGM-3A and BGM-7. ....	49

Figure 4-9	GWC-match base case (HIGHHP) of BGM-1 and BGM-7 (left) and water-production BGM-7 (right).....	49
Figure 4-10	Pressure match low vertical productivity case (INTERB_BELL033), P/Z curve (left) and deflection from straight line (right) BGM-1, BGM-3A and BGM-7.....	49
Figure 4-11	GWC-match low productivity case (INTERB_BELL033) of BGM-1 and BGM-7 (left) and water-production BGM-7 (right).....	50
Figure 4-12	Pressure match high productivity (INTERA_BELL080), P/Z curve (left) and deflection from straight line (right) BGM-1, BGM3A and BGM-7.....	50
Figure 4-13	GWC-match low productivity case (INTERA_BELL080) of BGM-1 and BGM-7 (left) and water-production BGM-7 (right).....	50
Figure 4-14	Pressure match aquifer case (LOWCUSHION), P/Z curve (left) and deflection from straight line (right) BGM-1, BGM-3A and BGM-7.....	51
Figure 4-15	GWC-match aquifer case (LOWCUSHION) of BGM-1 and BGM-7 (left) and water-production BGM-7 (right).....	51
Figure 4-16	3D model of seismic interpretation of Bergermeer, Groet and Bergen fields showing the only possible location of external aquifer is to the northwest of Bergermeer.....	53
Figure 4-17	Plot of water potentials [bar] in the blocks surrounding BGM for explicit aquifer scenario. The aquifer's connection with BGM is highlighted. The run shown is similar to the 'LowCushionX' run, but the aquifer strength and fault transmissibility were tuned to reproduce both the 100+ bar aquifer end pressure and the amount of water influx over the historic period, to indicate what the physical implications of the Fetkovich model are. Cf. Figure 4-18. Between the water blocks, all fault transmissibilities are unmultiplied.....	54
Figure 4-18	Pressure distribution (plotted is the water potential) and additional explicit aquifer attachment in the LowCushionX case. The fault transmissibility multiplier in the NW is set to a similar value as the BGM-7/BGM-main fault. Cf. Figure 4-17. Between the water blocks, all fault transmissibilities are un-multiplied.....	55
Figure 4-19	Aquifer inflow plot, LOWCUSHION case. It can be seen that aquifer influx does not reverse with cushion gas injection, which means the aquifer pressure is higher than the BGM reservoir pressure.....	56
Figure 4-20	Pressure match aquifer case (LOWCUSHION_REVERS), P/Z curve (left) and deflection from straight line (right) BGM-1, BGM-3A and BGM-7.....	56
Figure 4-21	GWC-match aquifer case (LOWCUSHION_REVERS) of BGM-1 and BGM-7 (left) and water-production BGM-7 (right).....	57
Figure 4-22	Pressure match aquifer case (LOWCUSHIONX), P/Z curve (left) and deflection from straight line (right) BGM-1, BGM-3A and BGM-7.....	57
Figure 4-23	GWC-match aquifer case (LOWCUSHIONX) of BGM-1 and BGM-7 (left) and water-production BGM-7 (right).....	57

Figure 4-24	Pressure match aquifer case (LOWCUSHIONY), P/Z curve (left) and deflection from straight line (right) BGM-1, BGM-3A and BGM-7. ....	58
Figure 4-25	GWC-match aquifer case (LOWCUSHIONY) of BGM-1 and BGM-7 (left) and water-production BGM-7 (right).....	58
Figure 4-26	Pressure match low productivity case (UBELL050), P/Z curve (left) and deflection from straight line (right) BGM-1, BGM-3A and BGM-7. ....	58
Figure 4-27	GWC-match low productivity case (UBELL050) of BGM-1 and BGM-7 (left) and water-production BGM-7 (right).....	59
Figure 4-28	Dynamic GWC maps at June 2007 of LOWCUSHION run (left) and base case, INTERA_BELL050 (right). Interestingly, while the GWC measured near the production wells is identical, aquifer influx has reduced the pore-volume in the north of BLOCK-2.....	60
Figure 4-29	Dynamic GWC maps at June 2007 of INTERB_BELL050 run (left) and HIGHP run (right). The INTERA and INTERB maps are very similar, but the HIGHP_ALT5_BFLS run shows increased local uplift of GWC near the best producers. The baffles in the MAIN block have similar transmissibilities. ....	61
Figure 5-1	Pressure vs. inventory plot per BGM-block. The dP between the production and injection cycles is caused by pressure-equilibration of the reservoir. The non-straight pressure is the average of the dP between straight and production, resp injection. The 40 consecutive UGS-cycles do not totally overlap due to a small production-injection imbalance. ....	67
Figure 5-2	Average reservoir pressure vs. time for base case UGS realisation (INTERA_BELL050). RPPG2 (black) is MAIN block, RPPG3 (red) is block-2. Cushion volume 5.5 Bscm, working gas 3.4 Bscm, 20 year forecast, 40 UGS cycles, 2 cycles per year with 72/88 day production/injection and rest periods between the cycles of ca 1 week.....	68
Figure 5-3	GWC behaviour UGS vs. HM of aquifer scenario INTERA_BELL050_LOWCUSHION. The GWC in BLOCK2 is actually pushed deeper than in the base case, but GWC-rise is higher in later cycles.....	70
Figure 5-4	GWC behaviour base case (INTERA_BELL050) at BGM-1, BGM3, BGM-3A and BGM-7 well-locations. Only BGM-7 is used in the UGS, BGM-3A is planned as water injector. In the ALT2 case BGM3 is in block1, in the ALT5 case, BGM3 is in block-2.....	70
Figure 5-5	Net reservoir height map between top ROSLU and original GWC at 2227 m, phase 2 base case (DISMIDHIGHKV_BELL050), which means the top is not uplifted to include seismic uncertainty of the INTERA/INTERB cases as used for phase 4.....	72
Figure 5-6	Depth of top ROSLU of the phase 2 model, DISMIDHIGHKV_BELL050 (colour scale limited to 2227 m). The top is not uplifted to include seismic uncertainty of the INTERA/INTERB cases as used for phase 4, which was later done to leave out the volume multiplier. ....	73

Figure 5-7	BGM-porosity logs. Wells flattened on TopROSLU. TVDss scale shown for BGM1 only, other wells have same relative scale.....	74
Figure 5-8	Intermediate phase 4 well-planning plotted on 'InterA' Top ROSLU-map with 5 m contours. Lower boundary is 2200 m tvdss (depth of horizontal wells). The horizontal wells cross the 200m distance to the fault (black line) and had to be re-orientated. ....	75
Figure 5-9	Phase 4 well-planning plotted on 'InterA' Top ROSLU-map with 5 m contours. The blue solid line indicates 'InterA' at 2200 m, almost coinciding with the 2200 m contour in this structure. (Cf. Figure 5-9.) [This top structure map is the one that was used in phases 1 & 2 for the base case; the current phase 4 horizons are shallower to get a volumetric match, see section 2.2. As emphasized there, the fact that the phase 4 horizons match the <i>overall</i> volumes better should not be read as implying that <i>locally</i> the shallower structure maps necessarily give a better prediction.].....	76
Figure 5-10	Same well pattern as Figure 5-8, but now on the seismic input base case top map.....	77
Figure 5-11	Cross-section through proposed UGS well HPROP34 displayed on BGM1 core porosity, model INTERA, vertical exaggeration 5. In addition the INTERB, HIGHP and base case horizons are also plotted. Cross-section is from NW (left) to SE (right). ....	78
Figure 5-12	Cross-section through proposed UGS well HPROP34 displayed on INTERA_BELL050 permeability, vertical exaggeration 5. In addition the INTERB, HIGHP case and base case horizons are also plotted. Cross-section is from NW (left) to SE (right). ....	78
Figure 5-13	NW/SE intersection (see inset). The well BGM9, between BGM6A and BGM-3A, does not penetrate the Rotliegend reservoir zone, as an illustration of the magnitude & areal length scale of top structure uncertainty. Shown is the seismic top (black) and the current model ('IntercaseB', pink), which due to smoothing & gridding resolution (100m) cannot honour this non-penetration. Also plotted are the ROSLU and ZEZ3G tops. Possibly in this case the structure reflects the impact of a fault corresponding to the 'BaffleN' in the model (Figure 4-3). [The BGM1 well is not exactly in the plane of the intersection, hence the apparent non-matching of tops.].....	79
Figure 5-14	Vertical location of the proposed horizontals HPROP31..36 for the three top structures used ('InterA', 'InterB', 'High', respectively). The RHS plot shows the core porosity trend (Figure 2-5) along with poroperm-based permeability logs for both BGM1 and BGM7. The scatter in the data suggests a range of trends: poor (green), base (purple; same as Figure 2-5) and high (blue). The latter seems to match BGM7 best, which is closest to the HPROP wells. ....	80
Figure 5-15	Static trend based estimates for the HPROP KH's in the 'InterA' top structure. ....	81

Figure 5-16	Static trend based estimates for the HPROP KH's using the 'base' vertical permeability trend.....	82
Figure 5-17	P <sub>res</sub> of base case 'INTERA_BELL050_ALT2' end of production cycle (left) and injection cycle (right). When interpreting this graph it should be remembered that the height of the HC column greatly varies across the structure. Thus the south-eastern (block I) area is much higher than the northern end of the field. In other words, the visual appearance of this plot can be misleading w.r.t. the volumetric importance of the various areas. ....	83
Figure 5-18	P <sub>reservoir</sub> low horizontal productivity case 'HIGHP_ALT5_BFLS' (left) and low vertical productivity case 'INTERB_BELL033_ALT5' (right) at the end of production cycle.....	84
Figure 5-19	Relationship between WBHP (wellbore pressure), WBP9 (pressure in connected and surrounding gridblocks and RPPG (reservoir pressure) for vertical UGS well (in block I), base case INTERA_BELL050. The skin for a vertical well is 20 (section 5.1.4).....	85
Figure 5-20	Differences between WBHP, WBP9 en WBP for horizontal well in Block-II, base case INTERA_BELL050. The skin for a horizontal well is 10 (section 5.1.4).....	85
Figure 5-21	Capacity losses in UGS with 1 production/injection cycle per year, rest periods of 90 days. Result is ca 4 bar loss in MAIN block, up to 16 bar loss after end of production cycle in the BGM-7 block. ....	86
Figure 5-22	Capacity losses in UGS with 2 production/injection cycles per year, rest periods of 8 days. Result is only 2 bar loss in MAIN block, up to 4 bar loss after end of injection cycle in the BGM-7 block.....	87
Figure 5-23	Pressure difference over northern baffle in MAIN block. The historical dP of ca 3 bar between BGM-6A and BGM-3A is increased to ca 15 bar during the UGS period, a multiplication of factor 5. The pressure plotted is well 9-gridblock-average pressures 'WBP9'.....	88
Figure 5-24	Comparison of non-tank behaviour in block averages pressure 'RPPG' (left) and well 9-gridblock-average pressures 'WBP9' (right). RPPG2=MAIN, RPPG3=BLOCK-2, red=block-I, green=block-II) vs. UGS gas-in-place. ....	89
Figure 5-25	Comparison of non-tank behaviour in well 9-gridblock-average pressures 'WBP9' between base case 'INTERA' 2 with cycles per year (left) and with 1 cycle (right). ....	89
Figure 5-26	Comparison of non-tank behaviour in well 9-gridblock-average pressures 'WBP9' between base case 'INTERA_BELL050' with ALT2 (left) and low vertical productivity model 'INTERB_BELL033' with ALT5 (right). ....	90

Figure 5-27	Effect of top structure on hysteretic behaviour. Plotted is an 'InterA' run (red) vs. 'InterB' run (blue). Dashed lines are block average pressures 'FPPG', full lines are 9-gridblock well average pressures 'WBP9'. The top plot shows block I, the bottom one block II. Clearly, the 'InterA' run (with more volume in the N, Figure 2-3), has more hysteresis in block II (approx. 15 bar vs. 10 bar). [The UGS rates are not identical in their relationship to the different block volumes, hence a small discrepancy in the absolute pressure levels. Also note that e.g. the relative sizes of the blocks are different in the two runs, so that certain other parameters, in particular the intra-field fault transmissibility multiplier, are different as well.] .....	91
Figure 5-28	Field capacity curves for UGS production cycle at 88, 110 and 133 bar, model BGM_INTERA_DISMID_ALT2_BELL050. ....	92
Figure 5-29	Historical WGR found during well tests in Bergermeer-wells. The higher values are found at lower rates, which shows the well was not properly cleaned out. ....	93
Figure 5-30	Comparison of historical WGR with expected values for UGS storage pressures, based on correlation charts from McKetta&Wehe [7].....	94
Figure 8-1	Original gas compositions BGM-1, liquid composition ALKM-1 and HICAL injection gas composition.....	104
Figure 8-2	Historical condensate production Bergermeer, back-allocated from gathering station of fields in Bergen concession.....	104
Figure 8-3	Historical condensate SG of fields in Bergen concession, initial SG is ca 0.8, this corresponds to SG 0.8005 (45.26 API of ALKM-1 @ s.c.) mentioned in PVT-report, Amoco, June 1994 .....	105
Figure 8-4	Bergermeer original gas composition (left), phase envelope (right).....	106
Figure 8-5	Mol-fraction distribution of UGS gas mixture at 1 <sup>st</sup> cycle.....	106
Figure 8-6	Condensate yield (CGR) of BGM UGS given at different initial pressures, e.g. at start of 1 <sup>st</sup> cycle (133 bara), a max. CGR of 2.5 sm <sup>3</sup> /MMsm <sup>3</sup> (0.45 stb/MMscf) is calculated. ....	107
Figure 8-7	Bergermeer UGS gas composition (left), phase envelope (right). ....	108



## Executive Summary

The present report documents the 4<sup>th</sup> phase of work on the sub-surface model of the Bergermeer field. This depleted gas field is scheduled for conversion to a UGS. In phase 1, the model was history matched, both w.r.t. pressure behavior and gas-water contact dynamics. During phase 2 the possible UGS scenarios were studied and in phase 3 the PVT description was looked at in more detail (see Appendix II of this report). The present work is focused on more detailed understanding of the behavior of the field when it will be converted to a UGS. To this end the most important well tests were explicitly modeled with the dynamic model, the geological uncertainty was more precisely captured and the proposed UGS wells were planned more in detail. The new constraint imposed by TNO, is a minimum distance between the future UGS-wells and the interpreted faults of 200 m.

During the summer of 2007 an injection test was executed in the Bergermeer field. This test has been interpreted during phase 2 [1]. The test highlighted that at the timescales of UGS operation the pressure behavior of the field may be more complicated than is evidenced by the production history. On the basis of this test some modifications were made to the subsurface model realizations. Additionally, well hydraulic modeling has been carried out. This, in combination with the updated subsurface model realizations, was used to generate capacity curves for the prospective Bergermeer UGS under various UGS conditions.

The main reservoir block, where most of the production wells are located is relatively well defined. The main reservoir uncertainty identified is the lack of definition in the North of the field and in particular in the western compartment (which contains only the BGM-7 well). Although the total volume in Bergermeer is precisely known, the compartment volume distribution is uncertain due to the unknown position of the main dividing fault; the reservoir quality is uncertain due to insufficient depth control of the top Rotliegend horizon. As was found in phase 2, it is expected that five horizontal wells need to be placed in block-2 in the UGS phase. The wells are needed to limit the pressure differential over the main fault, which has earlier proved to be non-sealing.

The uncertainty towards the North of the field, and the inability to put wells there from the surface facilities near BGM-1, poses the risk of a more adverse cushion gas/working gas ratio.

A further uncertainty is introduced by the remaining friction between well test permeabilities and history match permeabilities: previously the former covered a lower range than the latter, which were constrained by the GWC-match in BGM-1 in particular. After further, detailed, interpretation of the pressure transients in this phase, the two ranges do appear to overlap. The permeability uncertainty is captured by testing the UGS against multiple subsurface realizations, spanning the range from well test permeabilities to history match permeabilities. To keep a GWC match, in comparison to the previous work, the water leg permeabilities are lowered separately.

# 1 Introduction

The Bergermeer gas field is part of the onshore Bergen concession. The field has produced since 1971, from a gas accumulation that was initially estimated to hold about 17 BNm<sup>3</sup> originally in place, divided in two communicating compartments. It is nearing the end of its field life, and is currently considered for conversion to underground gas storage (UGS) facility. The location of the field is indicated in Figure 1-1.

During the first half of 2007, a modeling study was commissioned by Taqa Energy BV to explore the possibilities of converting the Bergermeer gas field into a gas storage. In the first phase of this study [1] a subsurface model for the field was built. This model was history matched, and some first steps were done to assess the behavior of the field under UGS conditions. In addition, the possibility of communication between the Bergermeer field (BGM) and its neighbors Groet (GRT) and Bergen (BER) was studied, as well as the reason for and impact of the water contact rise observed in Bergermeer (and Groet). Phase 2 of the study focused more on future UGS behavior. It was assessed how the subsurface uncertainties compare to well and other uncertainties. In addition, the injection test that took place during the summer of 2007 was interpreted, and its findings were incorporated.

During phase 3, the Bergermeer and future injection gas compositions were studied in more detail, a summary of this is given at the end of this report.

Phase 4 of the Bergermeer modeling study was commenced in the summer of 2008. Its focus was a more detailed well-planning of future UGS-wells. For this purpose well test-modeling was carried with the Eclipse model, thus closing the loop between well test interpretation and well-capacity modeling. New geological models were created with specific purpose to remove the pore-volume multiplier previously used. The model was also adapted to better model the horizontal UGS-wells projected in the west of the field. Concurrent to Phase4 reservoir modeling, a Drilling and Completion FEED was carried out for Bergermeer [3], giving more detail on well-design specifications.

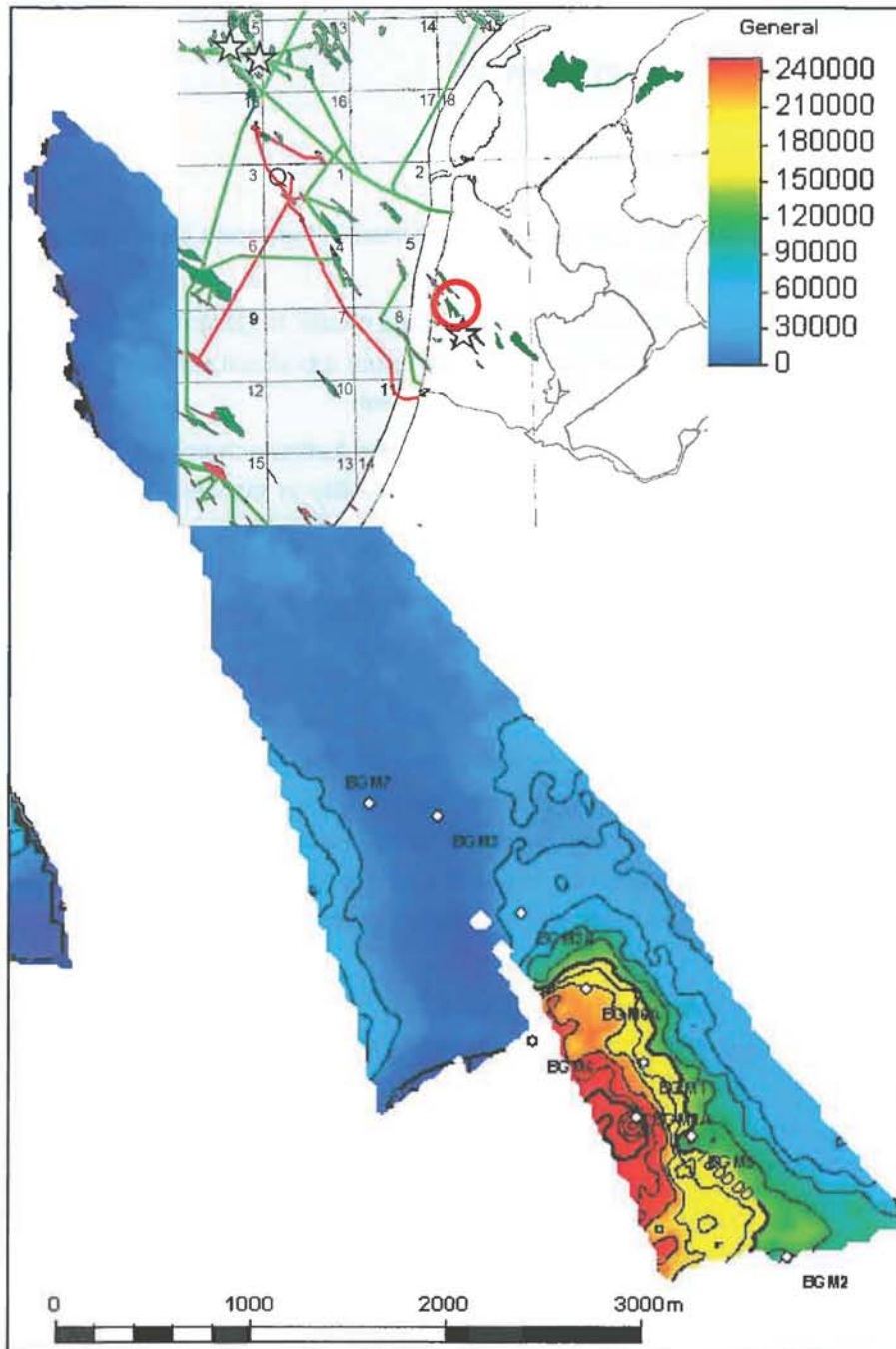


**Figure 1-1** Location of the Bergermeer field in the Bergen concession, projected on a KH-map [mDm] of the Bergermeer reservoir above the GWC-contact. The main UGS is in the southeast of the field, where also most of the production-wells are located.

## 2 Geological model adjustments

### 2.1 Phase 4 objectives

A detailed description of the Bergermeer field and model is contained in the report for the first and second phases of this study [1] and will not be repeated here.

Some of the objectives of phase 4 required revisiting the geological model. In particular, one of the objectives was to explicitly show that it would be possible to generate top structures such that the pore volume multiplier used in phase 1 and 2, could be dispensed with.

Moreover, in phase 4 the productivity of the forecast (UGS) wells was further scrutinized. This led to a detailed assessment of the vertical distribution of the permeability in the upper part of the 'ROSLU' Rotliegend reservoir zone (the zone sometimes called 'Weissliegend' [1]). These two issues will be discussed in the following sections.

### 2.2 Alternate top structures

In phase 1, a base case top structure map supplied by Taqa was used [1]. The volumes generated with this base case map in phase 1 and 2 were lower than the dynamic GIIP, such that a pore-volume multiplier of up to 1.19 was used. As it was thought that biggest volume uncertainty lies in the seismic top, new top structure maps were meant to correct for this PV-multiplier. The GIIP has a very low uncertainty as a consequence of the low remaining pressure in the field (i.e. as a consequence of the high recover factor).

Taqa provided an uncertainty map for the top structure (Figure 2-1). In phase 1, 'high' and 'low' top structures were generated by adding and subtracting, respectively, (the absolute value of) this uncertainty map from the base case map [1]. The pore volume multipliers need to match low/base/high case structures with the dynamic GIIP were 0.91 / 1.14 / 1.65 resp. [Note that the exact values depend to some extent (of the order 5%) on the property realization used.] This top structure variation was studied as a sensitivity both in the history match and the UGS forecast, driven by the following considerations:

- Is the static/dynamic GIIP discrepancy less than the static GIIP uncertainty? [answer: yes]
- Does the history match (HM) constrain *how* the discrepancy is resolved? [answer: no]
- Is the UGS forecast (FC) sensitive to *how* the discrepancy is resolved? [answer: no]

In phase 1 and 2 it was decided not to construct a scenario with MULTPV=1 given that the data made it obvious that such a scenario was possible, but the model behaviour made it unlikely that such a scenario would exhibit different responses.

However, the phase 4 work is targeted at a more detailed level, and therefore it was decided to construct such scenarios explicitly. The algorithm used is to incorporate the top structure uncertainty in a proportional way. Two alternatives were created:

- 'InterB': Top structure = Base (Phase 2) + 0.4 \* Abs(Seismic Uncertainty)
- 'InterA': Top structure = Base (Phase2) + InterA-map \* Abs(Seismic Uncertainty)

The InterA-map has a trend with multiplier of 1.0 in the north of the field, to 0.0 in the south of the field (Figure 2-2). The purpose of this map is to generate a scenario in which the highest proportion of the gas allowed by the top structure uncertainty is located as far away from the wells as possible. *If* the dynamic reservoir behaviour is sensitive to the top structure uncertainty, this map would be a likely candidate for exhibiting it.

In both of these scenarios, the 'discontinuous mid' property model was used [1], the seed number of which was iterated to give a close match of the dynamic GIIP. In addition to these two scenarios, a third alternate was developed:

- 'HighP': Top structure = Base (Phase2) + 1.0 \* Abs(Seismic Uncertainty)

This was to get a match on the volume in this scenario the (vertical) porosity distribution was modified. This porosity distribution will be discussed in more detail in the next section. It should be noted that in these scenarios the neighbouring fields Bergen (BER) and Groet (GRT) have incorrect volumes. Since these were not the focus of the phase 4 work, this was not further considered.

Furthermore, it should be emphasized that the scenarios chosen were aimed at testing the limits of dynamic behaviour, and emphasize *overall* top structure uncertainties. This means that the spread between these scenarios at any *specific* location is not an indication of the *local* uncertainty there; i.e. these scenarios cannot be used to capture the risks for (horizontal) well placement.

Moreover, the scenarios generated are aimed at dynamics only; they are to some extent artificial, and they are not properly geologically and geophysically constrained. A proper (geophysics) study into the sources of this uncertainty, e.g. with the aim of generating a sequence of 'equiprobable' top structure realizations, was outside the scope of this phase 4 study.

As a final caveat; note that the present work was done in the 2008 version of Petrel, whereas the original work was done in the 2005 version. Some differences in local well corrections are a result of this. Moreover, the extrapolation towards the faults is not handled 100% consistently in these scenarios, but since this did not critically affect their aim, this was not corrected.

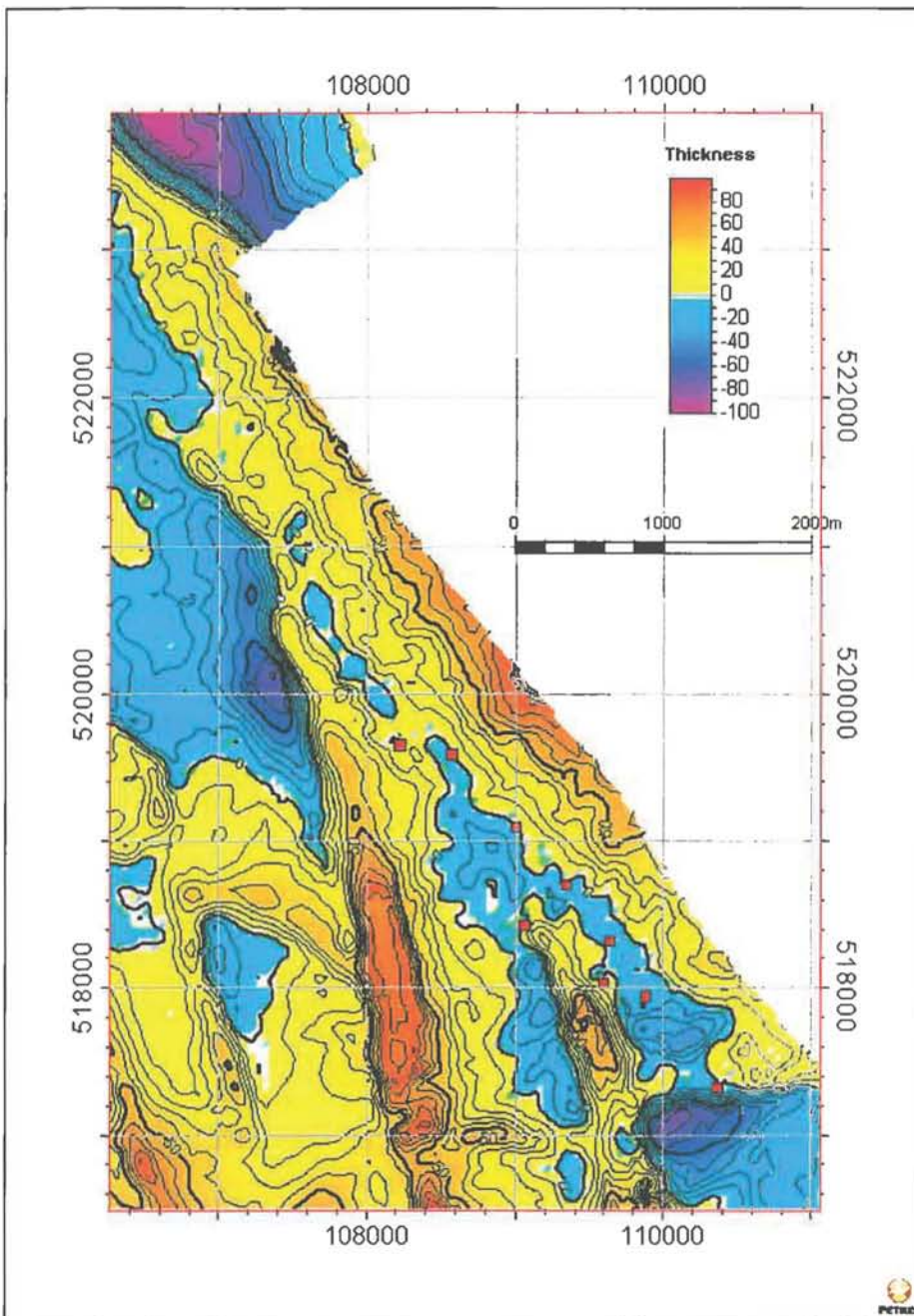


**Figure 2-1** Uncertainty map for Top ROSLU. Uncertainty is expressed in m, top ROSLU well picks are plotted as red squares.

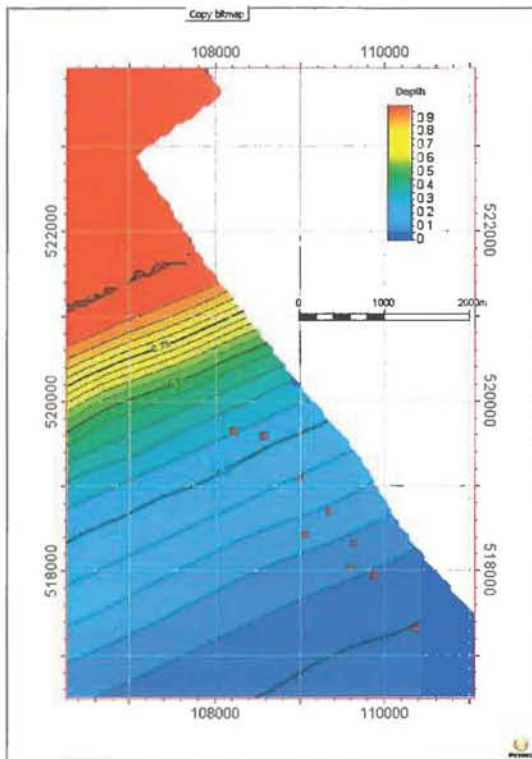


**Figure 2-2** 'InterA' uncertainty proportion trend map, ranging from multiplier 1.0 in the north to 0.0 in the south. For reference the top ROSLU well picks are plotted as well (cf. Figure 2-1).

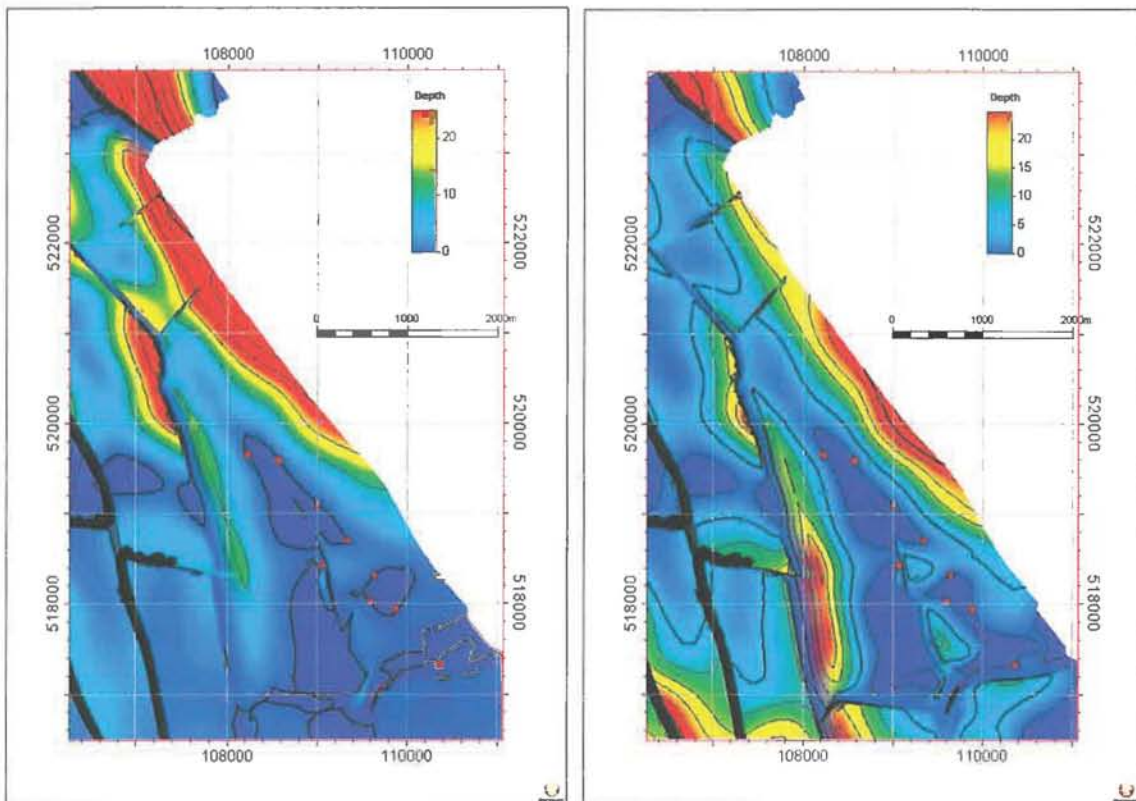


**Figure 2-3** 'InterA' (left) and 'InterB' (right) uplifts w.r.t. base structure maps. Offset is in m, red squares mark top ROSLU well picks. The maps are smoother than the input uncertainty map as a result of the Petrel gridding process [1].

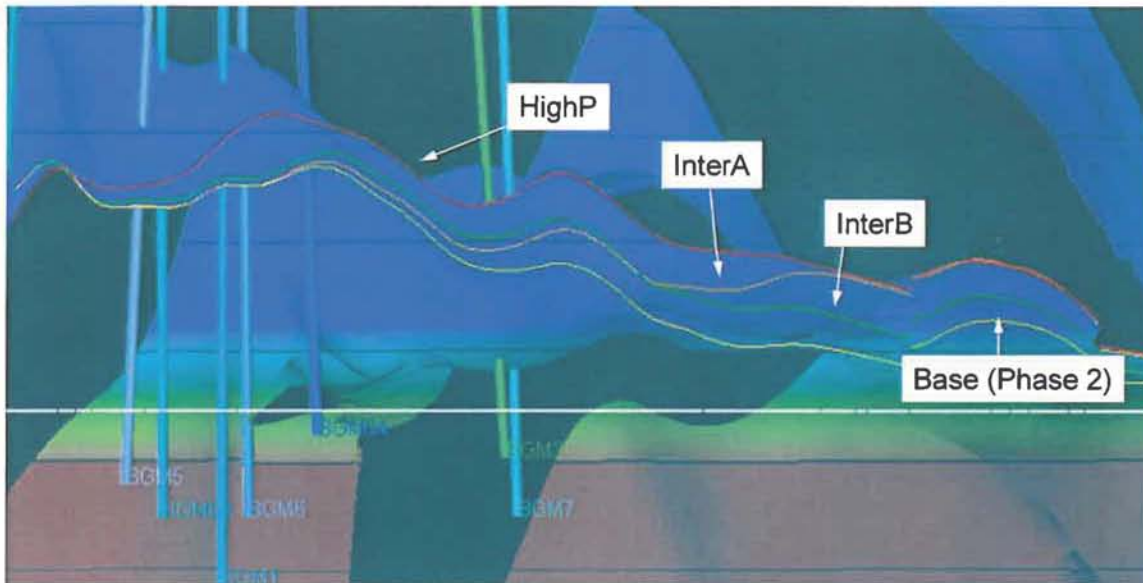


**Figure 2-4** NS section of the field, just East of BGM1, viewed from the East. The yellow line indicates the base top structure according to seismic interpretation, the white line the original GWC. The cross-section highlights some extrapolation issues towards the eastern boundary fault (in the H case vs. the others). These are caused by the fact that the Petrel mapping & well correction are not 100% controllable; nevertheless overall fractions are honored.

## 2.3 Vertical reservoir quality distribution

A key factor in assessing the behaviour of the Bergermeer field is the contrast between the upper and centre reservoir zones, as exemplified by the performance of the BGM7 and BGM1 wells. As can be seen in Figure 2-5, the porosity increase from the top ROSLU downwards shows a steep trend of 8.6% / m. This, as we shall see, is of importance for the placement of the horizontal wells in the UGS: the top structure uncertainty maps to a large permeability uncertainty if we keep the well depths fixed. We will discuss this in more detail in section 5.4.

As discussed in the phase 1 report [1], the 'discontinuous mid' property model had the inappropriate property that the upper part of the Rotliegend the properties were too good, as a consequence of the fact that the short variogram range was applied to the vertical permeability trend as well as to the 'poor streaks'. But the vertical deterioration appears more correlatable than the 'dismid' model assumes (Figure 2-6), although the deterioration does show some spread (in particular BGM7 appears better than BGM1; Figure 2-7).

To address this, an adhoc 'Bell' multiplier was used to reduce the upper reservoir zone permeabilities compared to the center reservoir zone. Moreover, the well->geocellular->dynamic upscaling resulted in kv/kh ratios that were lower than observed in the well tests. Therefore a weighted averaging of kv and kh was done. The resulting 'DISMID\_HIGHKV\_BELL050' scenario was used as the base case scenario in the phase 2 simulations [1].

Still, this scenario tends to overestimate the permeability in the uppermost reservoir zone (Figure 2-11). Moreover, the application of an adhoc multiplier like this is somewhat unsatisfactory, especially since the corresponding correction to the poroperm is not made (or, in other words, the top reservoir zone has a more pessimistic poroperm). As it was found that the top reservoir zone



permeabilities are particularly important for the project, we recommend that, if follow-up work takes place, this is analyzed in more detail.

To get an idea of where such analysis would lead, a realization was built in which the upward deterioration is modeled more strictly already in the porosity (in Petrel-technical terms, a vertical trend function was replaced by a data analysis trend). The resulting permeabilities are shown in Figure 2-12. As the porosities in the upper reservoir zone are poorer in this model, and since the upper reservoir zone contains a significant portion of the case, this porosity/permeability model needs to be combined with a fully uplifted top structure in order to make the static volumes match the dynamic ones. This high structure/poor top combination is called 'HIGHP'.

In the context of this QC it was found that the porosity log used in a few wells (BGM1 and BGM8) was not 100% aligned with the procedure discussed in the phase1 report. This oversight was corrected.

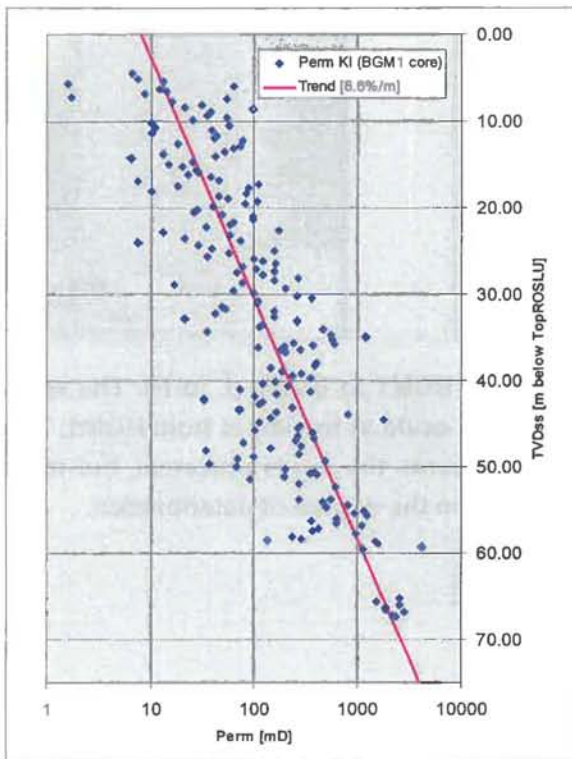


**Figure 2-5** BGM1 core permeabilities (Klinkenberg-corrected) vs. distance from top reservoir. The data exhibits a steep exponential trend with a porosity increase of about 8.6 % per m from top ROSLU downwards.

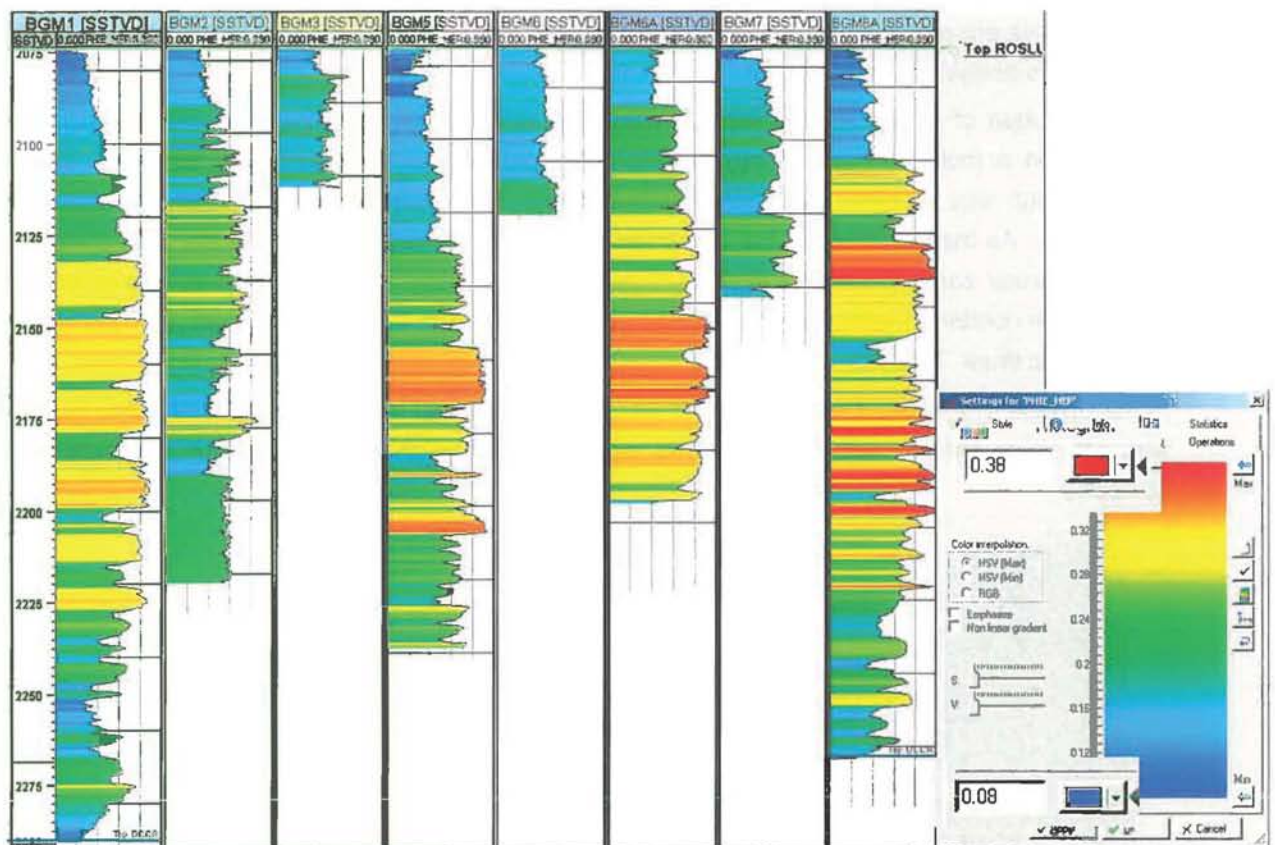


Figure 2-6 Correlation panel for the PHIE log from BGM1 to BGM8 (L to R). The wells are aligned at the top ROSLU, the depth scale at the left is from BGM1. The deterioration of the reservoir quality towards the top is universal, but there are quantitatively significant differences in the degree of deterioration.

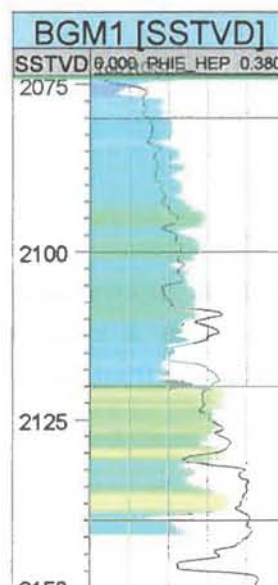
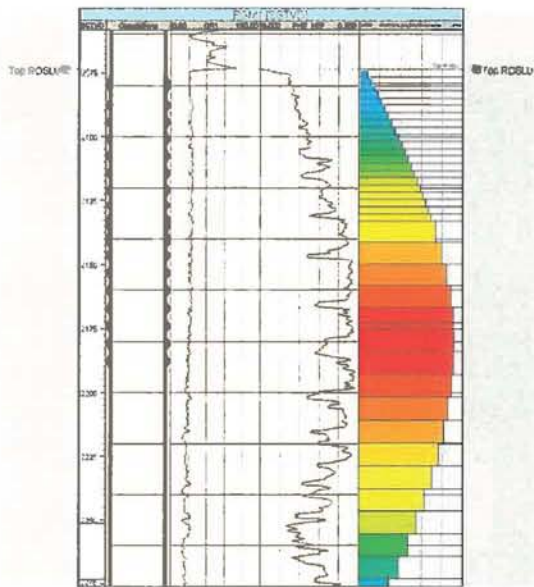
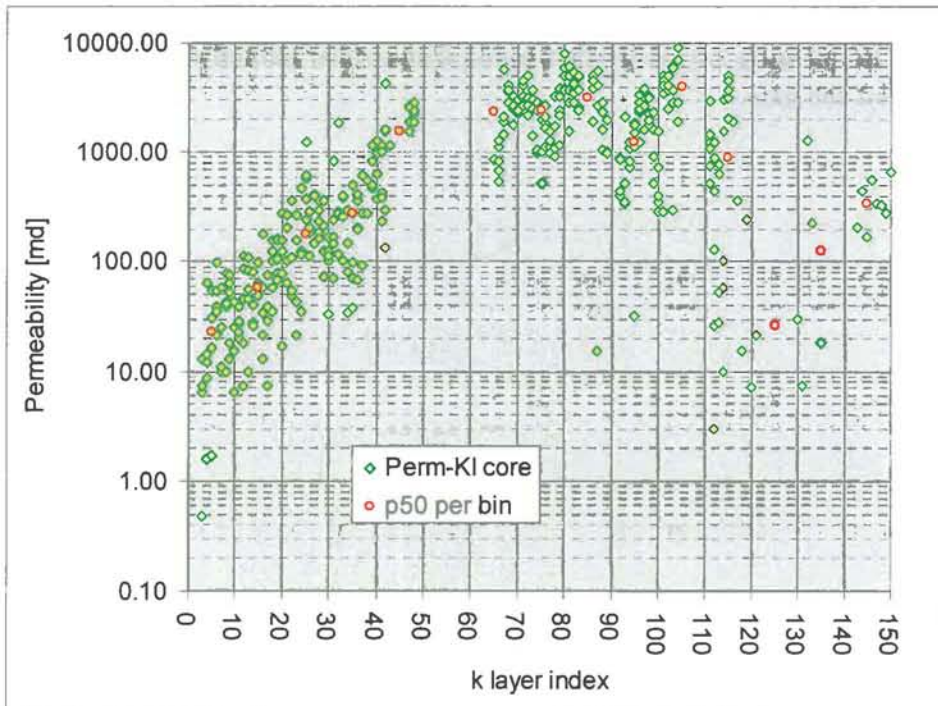


Figure 2-7 Overlay of the PHIE logs of BGM1 (line) to BGM7 (colours). The wells are aligned at the top ROSLU, depth scale is from BGM1. Both wells show a deterioration of the reservoir quality to the top, but at relevant depths BGM7 is several (4) PU's better, which maps to significantly higher permeabilities for the porperm used (factor 5).



**Figure 2-8** Bell multiplier profile plotted along the BGM1 track. Top reservoir is indicated, as is the GR and PHIE log, as well as the (final) perforation status. The 'BELL050' curve has, in combination with an overall multiplier from matching to well test KH's (chapter 3), the value 0.5 in the centre, 0.15 at the top.



**Figure 2-9** Plot of BGM1 Klinkenberg-corrected core permeability vs. k-layer index in the static model (which has 150 layers). The core permeabilities are binned by groups of 10 k layers; the P50 of each bin is also plotted.

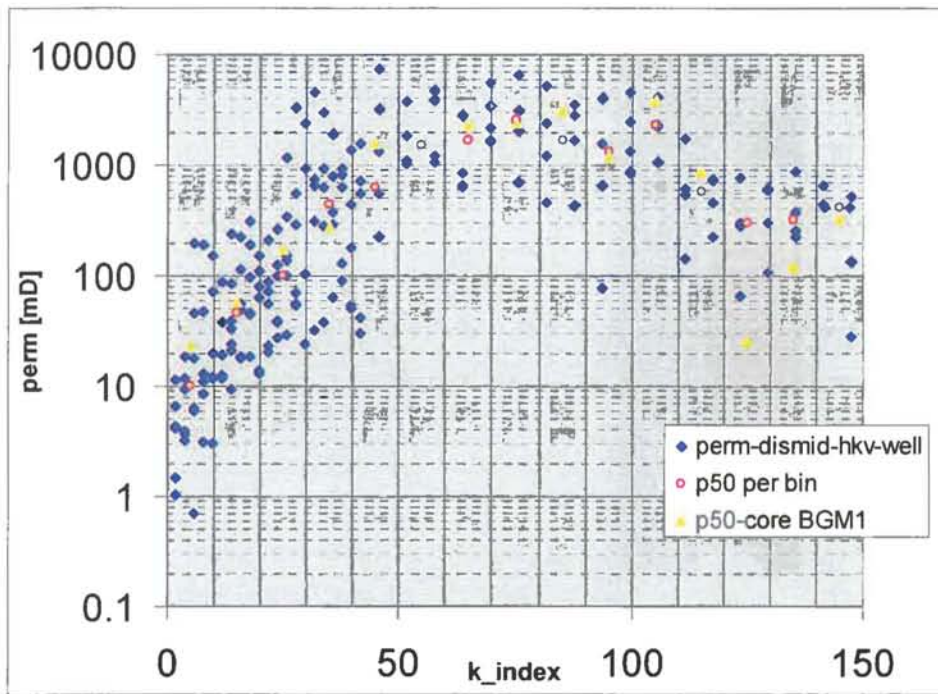


**Figure 2-10** Permeability in dynamic model cells that have (PHIE) log values as their base (i.e. where the fine static model has ‘upscaled cells’). No multiplier has been applied, apart from the ‘khkv’ correction (see above). The binned core values from Figure 2-9 are plotted, along with similar binned values of the upscaled cell data.

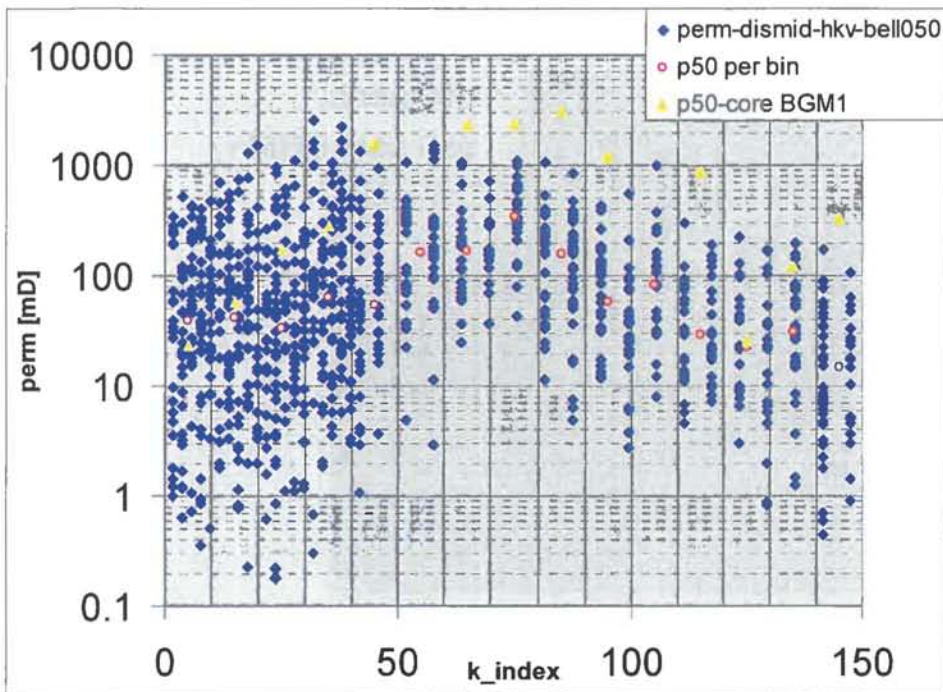


**Figure 2-11** Permeability in the 'BELL050' dynamic model vs. static model K index. The 'BELL050' multiplier includes well-test based correction (Figure 2-8). The binned core values from Figure 2-9 are plotted, along with similar binned values of the cell data.

The profile is more conservative than core & well data (Figure 2-9, Figure 2-10), except for the top 15 m of the reservoir (the top 10 fine K layers). Note the vertical alignment of the points indicating the finer simulation grid at the top (section 2.4).

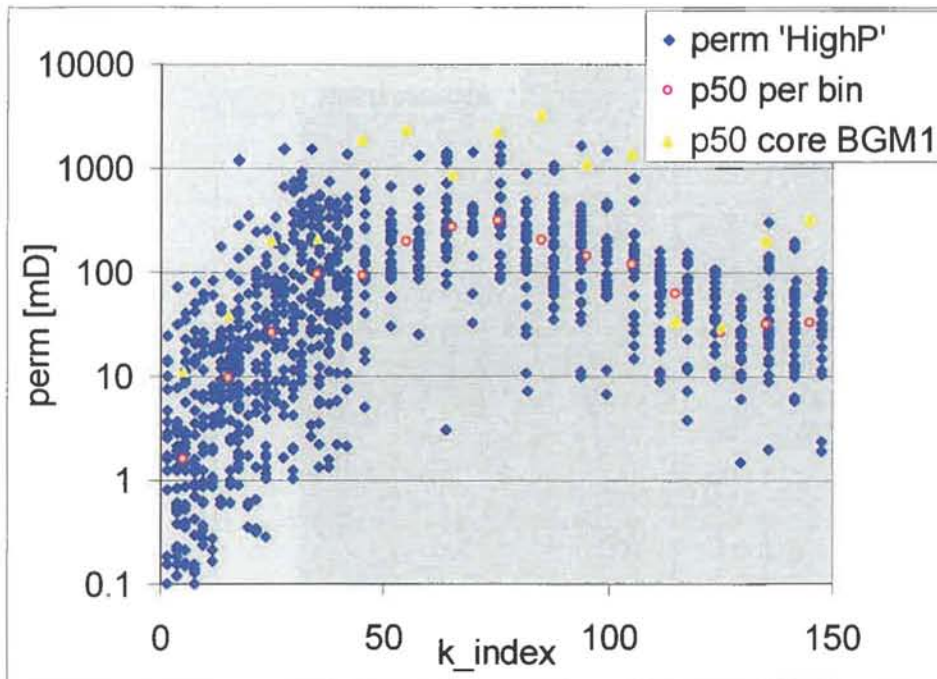


**Figure 2-12** Permeability in the ‘HIGHP’ dynamic model vs. static model K index. The ‘HIGHP’ permeability includes a well-test based correction (Figure 2-8). The binned core values from Figure 2-9 are plotted, along with similar binned values of the cell data. The profile is more conservative than core & well data (Figure 2-9, Figure 2-10), as a consequence of well test matching, and honours the core trend in the top 15 m of the reservoir (the top 10 fine K layers). Moreover, the scatter around the trend is less. The ‘HIGHP’-porosity also deteriorates more steeply towards the top. Note the vertical alignment of the points indicating the finer simulation grid in the upper reservoir section (see section 2.4).

## 2.4 Upscaling / grid dimensions

The upper part of the reservoir (ca 58 m) was refined to be more accurate on the fluid distribution near the future horizontal wells. Here, the gridblock-height was reduced from ca 8.4 m to ca 2.8 m, which was attained by upscaling the static grid in Petrel by 1:2 in the top and 1:6 in the rest of the reservoir. The number of k-layers increased from 24 to 41. For most UGS runs, the Groet and Bergen parts of the model were left out, further reducing the amount of gridblocks. No areal upscaling was used, leaving the gridblock-size laterally at 100 x 100 m. The dimensions of the BGM-model are 58 x 182 x 39 (411.684 grid-blocks).

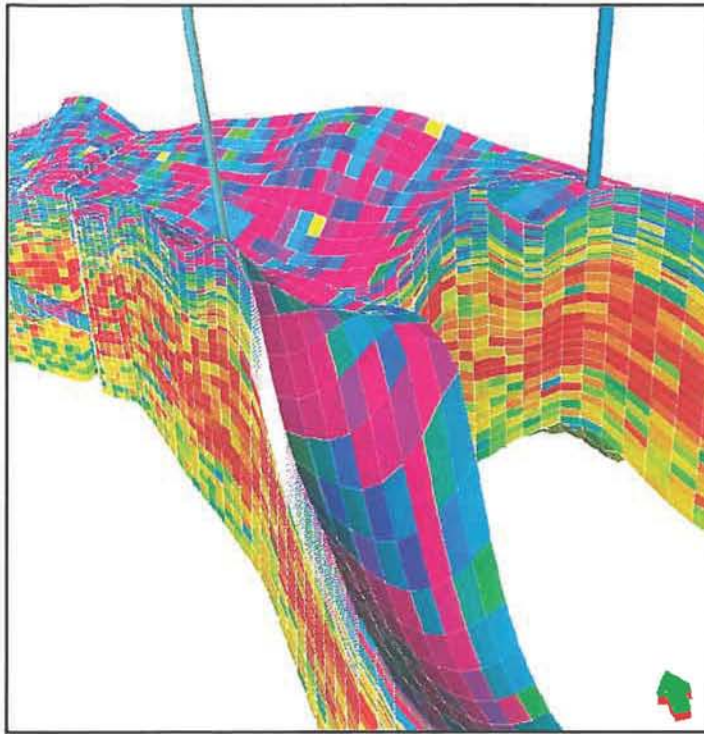


**Figure 2-13** View of porosity in upscaled grid with BGM-7 (left) and BGM-6A (right).

Figure 2-13 shows the locations of BGM-6A and BGM-7 in the grid. The flank left of BGM-7 is slightly uplifted compared to the rest of Block-2. Although the best porosities are still located beneath the GWC in this block, the horizontal UGS-wells are targeted at this structural high to optimize KH and keep away from the GWC as much as possible. See section 2.3 for details on the porosity and permeability trends.

### 3 Well test modeling

#### 3.1 Introduction

The well tests that were carried out in Bergermeer have already been revisited for Phase 2 of the modeling study. The main purpose of the re-interpretation was to resolve remaining questions regarding rate-dependant skin and reservoir permeability. As the well tests were always carried out for capacity-checking purposes, not to increase knowledge of the reservoir, they are not suitable for detailed interpretation, such as the possible location of boundaries.

For Phase 4, the most important well tests in BGM-1 and BGM-7 were modelled directly in Eclipse, in order to check interpretation results and see if model parameters are in agreement with Pressure Transient Analysis results. Initial matching was done with Phase 2 models; later, the matches were revisited to incorporate Phase 4 model changes.

#### 3.2 Core permeability averages

Well Test permeability is often compared with one of the core plug averages: arithmetic, geometric and harmonic. A question that often arises is which average does the well test-derived permeability represent and over what region is this average valid? A second important question is how should the data sets be reconciled when there are discrepancies? In practice, the permeability derived from well tests is often assumed to be equivalent to the arithmetic average (of the plug measurements) in a layered reservoir or geometric in a randomly distributed permeability field.

The BGM-1 core permeability values are given per ft. Upscaling takes place from core to the Petrel voxel-grid and from the voxel-grid to the dynamic model. The voxel grid has average gridblock height of ca 1.6 m or 5 ft (factor 5), while the dynamic model again has factor 5 upscaling to get ca 8 m (26 ft) high gridblocks. While porosity was upscaled arithmetically in Petrel, the permeabilities were upscaled using the 'diagonal tensor' method, a combination of the arithmetic and harmonic average, which produces higher averages than geometric upscaling.

For the Bergermeer static model, geometric upscaling in Petrel would have produced much lower permeabilities than the tensor method. Table 3-1 shows that the permeability over the 1997 perforation interval would have been much lower than the well test-average (see Table 3-2). As the main Rotliegend reservoir has randomly distributed low permeability-streaks, this would have been plausible.

BGM-1		
	Perf-height [m]	Perm [mD]
1969	17	783
1987	57	133.2
1997	115.6	275.4

\*Core average permeability, geometric mean, 90% scaled

**Table 3-1 BGM-1 average core permeability, geometric mean, 90% scaled.**



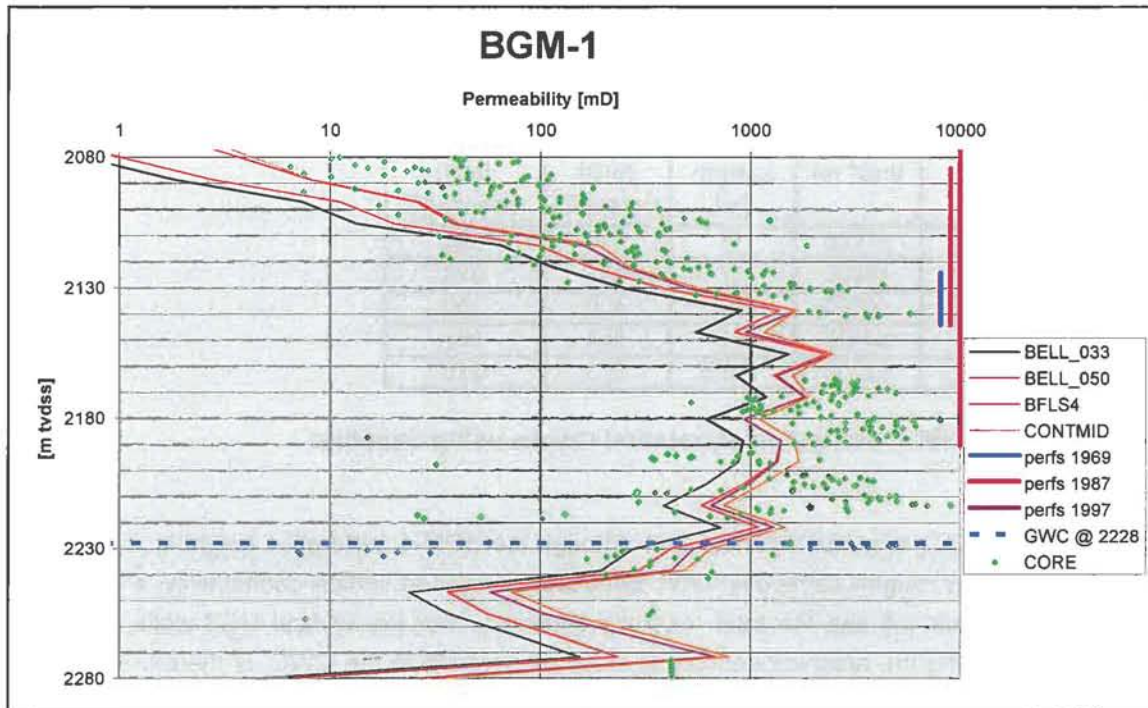


**Figure 3-1 BGM-1 core permeability vs. Phase 2 model permeability. Model average permeability is upscaled in Petrel using the diagonal tensor method (harm/arithm.) Note that the best section has no core coverage due to the unconsolidated nature of the section.**

Figure 3-1 shows the permeability of the Phase 2 models vs. the raw core data with depth. As discussed above, the model is on the conservative side compared with core due to upscaling algorithms in Petrel. This is especially the case for the upper part of the reservoir (the so-called 'Weissliegend') due to the BELL-shaped multipliers  $<1$  for the top and bottom of the reservoir.

### 3.3 Reservoir height as seen by well tests

Table 3-2 gives the KH of BGM-1 in the main block as one of the well test interpretation results using Sapphire (see also Table 2.5 in the Phase 2 report). In order to obtain the average permeability from KH, it is traditionally divided by the total reservoir thickness, which is 155 m in the case of BGM-1. It is believed that this is probably a too conservative approach. The top of the Rotliegend (sometimes called 'Weissliegend'.) has much lower porosity and permeability than the main Rotliegend reservoir. The deterioration of the top reservoir on a field-wide scale in Bergermeer, the height of this zone is roughly between 30 and 50 meters (see Figure 2-6). Discounting the KH for this zone for BGM-1, the well test permeability as found by well test interpretation is some 55% higher. Although horizontal low-permeability-streaks exist both in the top zone and in the lower parts, it is believed that the radius-of-influence during the test is greater than the extent of the low-permeability-streaks. The streaks were believed to be non-continuous with extent of max 100m [1]. For the BGM-7 block, where only the top Rotliegend is above the

GWC, the well test radius of influence is much smaller and the low-perm streaks are believed to be also horizontal barriers during the well test. This is explained in modeling of the BGM-7 well tests later in this section.

Well	Date	KH [mD* m]	Perf. Length [m]	K [mD] Hres=100	K [mD] Hres=155
BGM1	1986	61000	17	610	394
BGM1	1987	48000	57	480	310
BGM1	1990	40000	57	400	258
BGM1	1996	54425	57	544	351
BGM1	1997	57300	116.5	573	370

**Table 3-2 BGM-1 well test interpretation results using Sapphire.**

Looking at Table 3-2, it is import to note that although the BGM-1 perforation height increases, the KH of BGM-1 stays roughly same over time. Because of the good vertical connectivity, a well in the Rotliegend reservoir will see the total reservoir thickness. For the vertical UGS-wells, the main reason for extending the reservoir-section as close as possible to the GWC, is therefore mainly a decrease in the mechanical and rate-dependent well-skins.

[deleted text because of confidentiality]

**Table 3-3 Well test-KH from latest test in existing BGM-wells, taken from Phase2 report Table 2-5 and Table2-6. The value for BGM-7 is the drawdown-KH (BU-KH is 330 mDm). (\*) was previously interpreted by TAQA.**

The well test-KH from the existing BGM-wells (see

Table 3-3) was compared with the KH in the dynamic models used for Phase4, see Figure 3-15. Plotted in the graph are the model KH's over the full reservoir zone (TopROSLU-GWC), no rlp effects are included. Still, the model-KH is for almost all wells higher than the well test-KH. There are several reasons to explain this. Firstly, in reality, no full penetration is present; the top ROSLU section should be deducted from the values in the plot. For BGM-8A, the well test-value is much lower than for earlier tests and probably influenced by sand-problems. The value for BGM-3A is just below the 1000mDm line, but because the well has no logs, the permeability could not be constrained at this place. BGM6A has unreliable logs (no density log was run, and sonic/density porosity calibration was deemed insufficiently reliable) and was therefore not used in population of the geological model. BGM-2 is very close to a fault, and the well test-KH probably over-represents the degraded fault-zone with respect to the well-logs. For the BELL033 and BELL080 models, the values are just 2/3 and 8/5 of BELL050.

### 3.4 Well test modeling with Eclipse dynamic model

For Phase 4, the most important well tests in BGM-1 and BGM-7 were modeled directly in Eclipse, in order to check interpretation results and see if model parameters are in agreement with Pressure Transient Analysis results. Initial matching was done with Phase 2 models; later, the matches were revisited to incorporate Phase 4 model changes. The goal was to compare the log-log plots from well test-interpretation using Sapphire with the log-log plot derived from the dynamic model. To do this, new Eclipse-decks were built using the existing dynamic models. A specially built Xcel-macro was used to compare the log-log plots of the historical data with the modeled data.

The following steps were undertaken to set the Eclipse-deck for well test modeling:

- Set up production rate history file of well test
- Initialise model at historical pressure and GWC at the well test-date
- Apply LGR around the wellbore
- Re-define and re-position the well in middle of LGR
- Apply wellbore volume for correcting the early time pressure behaviour
- Tune the timesteps and linear and non-linear iterations for convergence of the model

The LGR was defined radially, using number of circles = 20, Nr of quadrants= 4. Vertically, the refinement was a factor 8, so that the vertical cell thickness is roughly 1 m. This refinement gives for example  $20 \times 4 \times 8 \times 7 = 4480$  cells for the BGM-1 well test of 1987.

After running the model, the output data was manipulated in MS-Xcel to extract the time and pressure derivatives for the log-log plot. This was then compared to pressure and time derivatives of the well test.

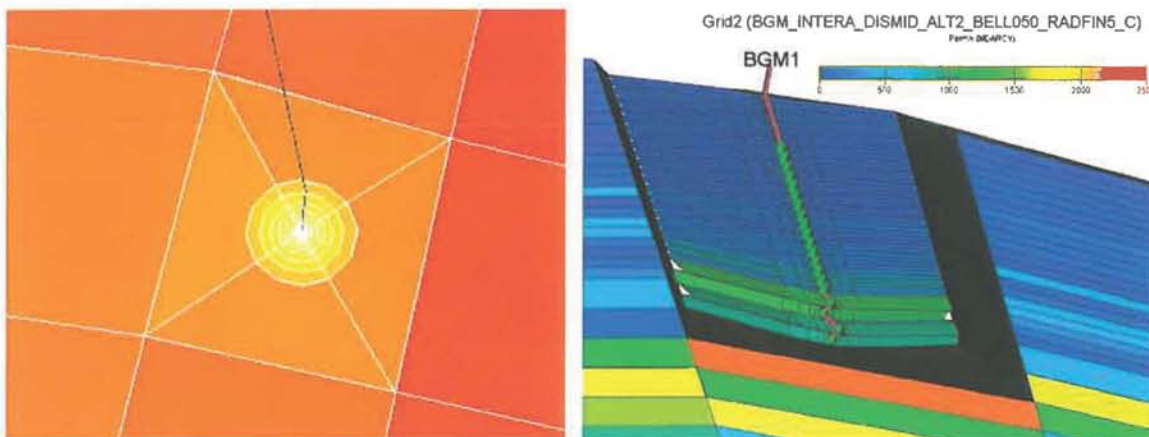


**Figure 3-2 Radial LGR of BGM-1, with NR=20, Theta=4, top view (left) and cross-section of 3D permeability model with range 0 – 2500 mD (right).**

## 3.5 BGM-1 well test modeling results

Three well-tests were simulated dynamically with Eclipse. The reason for this is that the perforation height has changed in time from 17m in the 1986 test to 116 m in the 1997 well test, which almost covered the whole reservoir section. It was observed that Eclipse handles the partial penetration effects differently than Sapphire. Also the mechanical skin and rate-dependent skin factors are not one-to-one comparable with well test interpretation results. The KH calculated by Eclipse from the perforation height had to be adjusted to get the correct drawdowns. The permeability-multipliers that were used ranged between 0.78 and 1.47 for the high, resp. low case UGS productivity models, which indicated that the permeability of the different UGS scenarios is in the correct range. The absolute KH, matched with the Eclipse models, does however not seem to be totally consistent with the KH from PTA (Pressure Transient Analysis), see Table 3-4.

### 3.5.1 BGM-1 well test 1986

The multi-rate test from 1986 was modeled with the base case geological model 'BAG25\_ALT2\_DISMIDHIGHKV\_BELL050'. Both the drawdown plot and the log-log plot could be well-matched. Like in the well test, only the top 17 m ROSLU section was perforated, see Figure 3-1. The match results can be summarised as:

- KH = 21500 mDm\* (BU#5)
- PERM-mult = 1.47 (BELL\_050)
- Perf-height = 16.6 m
- Kav = 1292 mD
- WDFAC = 17E-6 day/sm<sup>3</sup>

It can be seen that the modeled KH is lower than the well test-KH from PTA analysis of ca 57000 mDm. The permeability from the base case model (BELL\_050) had to be multiplied with a factor of ca 1.5. The D-factor is a bit lower than the value of 20 [MM m<sup>3</sup>/d]<sup>-1</sup> for the base case UGS, see also section 3.3 of the Phase2 report. The value is about half the value from PTA analysis, where 35 [MM m<sup>3</sup>/d]<sup>-1</sup> was found. Note that both the drawdowns and build-ups are equally well-matched, see Figure 3-3.

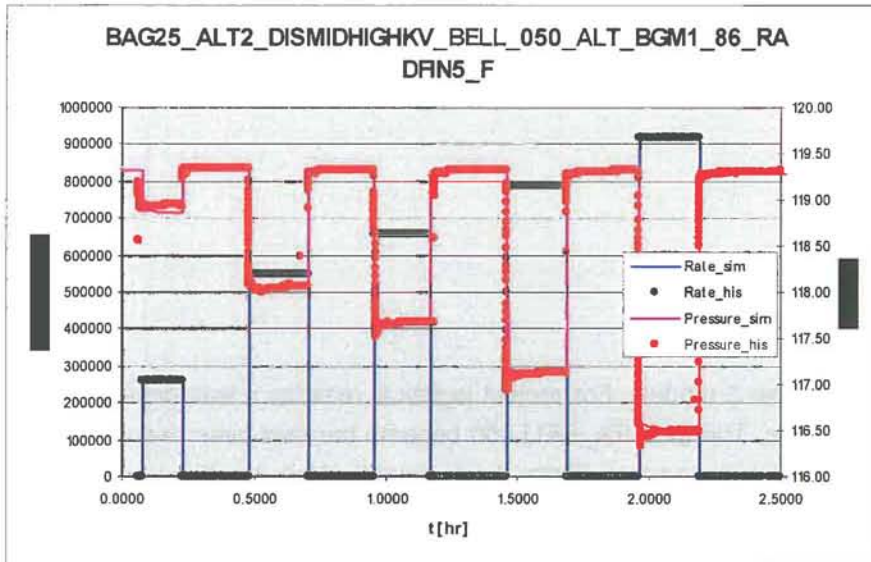


**Figure 3-3 Match of BGM-1 well test from 1986 with phase2 base case UGS model, rate (left) and pressure (right) vs. time (hours).**

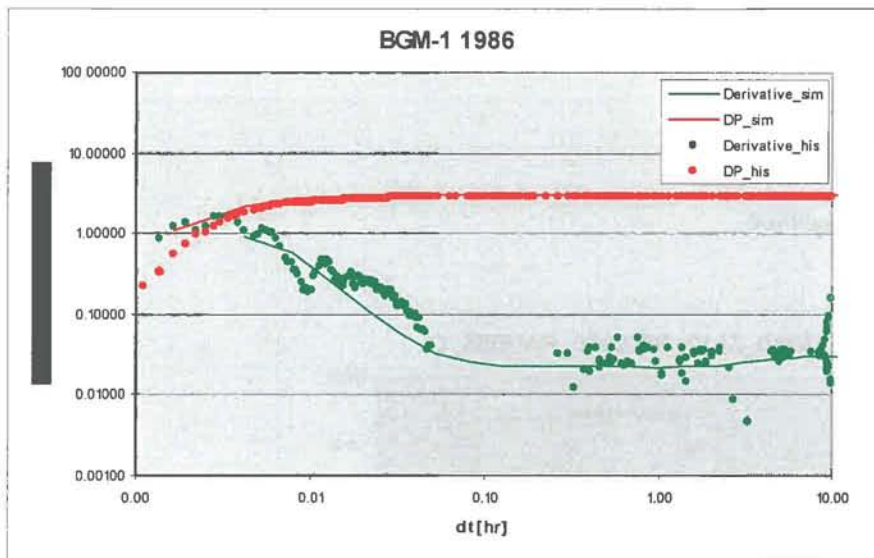


**Figure 3-4 Match of BGM-1 well test from 1986 with phase2 base case UGS model, log-log-plot.**

### 3.5.2 BGM-1 well test 1987

The perforated height was increased from 17 to some 58 m just before this test was done. For the interpretation of this test, not only the base case, but also the low (BELL\_033) and high productivity (WDF\_BFLS4) models were considered. The KH for a well test-match was the same for all models, but as the permeability was not, the multipliers used were 1.47 for the BELL\_033, 1.0 for the BELL\_050 and 0.7825 for the WDF\_BFLS4. The D-factor was higher than previously interpreted. The main results of the base case match (BELL050) are:

- KH = 24005 mDm (BU#4)
- Perm\_mult = 1.0
- Perf-height = 58.2 m
- K = 412 mD (Hres 58m)
- WDFACCOR = 2.7E-6 [day/sm3]

The matching was done on phase 2 models. For project logistical reasons it was decided to only re-run for the phase 4 base case. The INTERA\_BELL050 became the new base case and had a refined grid in the top ca 60 m reservoir section (factor 3 refinement). While the KH did not change significantly, the D-factor keyword was changed from WDFACCOR to WDFAC as this was also the keyword used for the UGS models. The new match-value is 14 / MM day/sm3, which is lower than the 1986 test (17 MM day/sm3). The main results are:

- KH = 20005 mDm (BU#4)
- Perm mult = 1.0
- Perf-height = 58.2 m
- K = 344 mD (Hres 58m)
- WDFAC = 14E-6 [day/sm3]

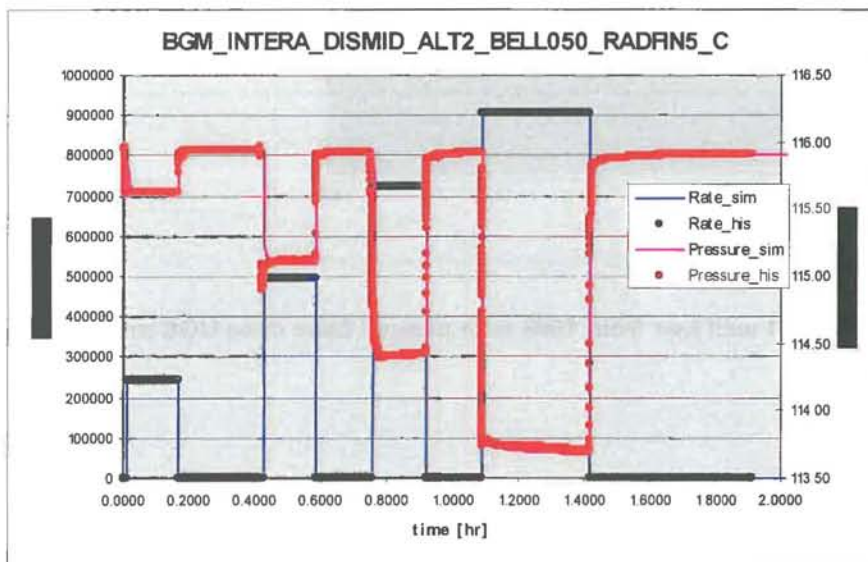


**Figure 3-5 Match of BGM-1 well test from 1987 with base case UGS model, rate (left) and pressure (right) vs. time (hours).**

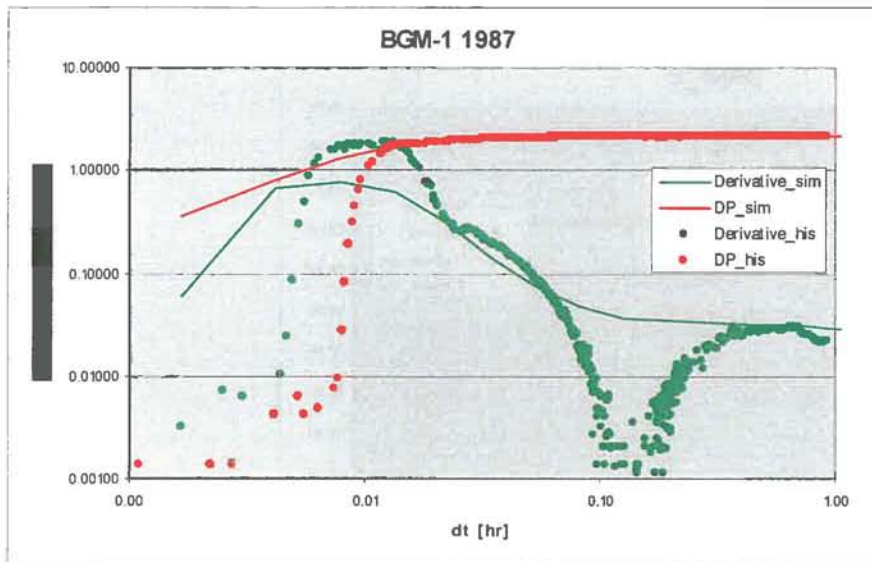


**Figure 3-6 Match of BGM-1 well test from 1987 with base case UGS model, log-log-plot.**

### 3.5.3 BGM-1 well test 1997

The 1997 well test was done on a fully perforated reservoir section. While PTA analysis took the last build-up for analysis, for Eclipse the more stable first BU was modeled. Both the permeability and the non-Darcy values modeled in Eclipse are conform values found by PTA analysis. The KH-values for PTA / Eclipse are 57300 / 52374 mDm and for the D-factor 17 / 16 per MM d/sm<sup>3</sup>. To obtain the KH in Eclipse, the permeability had to be multiplied by 0.53. This indicates that the permeability in the model could be too high. With a multiplier for the base case model of 1.5 for the 1986-test and 1.0 for the 1987-test, the 1997-test completes the range at the low end. A summary of the results is given below:

- KH = 52374 mDm (BU#1)
- PERM-mult = 0.53 (BELL\_050)
- Perf-height = 116.0 m
- K = 455 mD (Hres 116 m)
- GWC @ 2214 m tvdss
- WDFAC = 16E-6 [d/sm<sup>3</sup>]

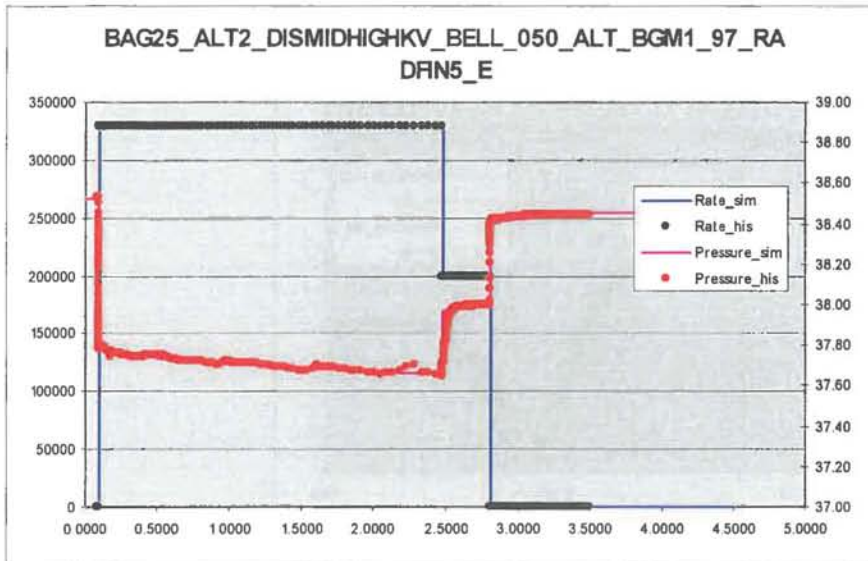


**Figure 3-7 Match of BGM-1 well test from 1997 with phase2 base case UGS model, rate (left) and pressure (right) vs. time (hours).**

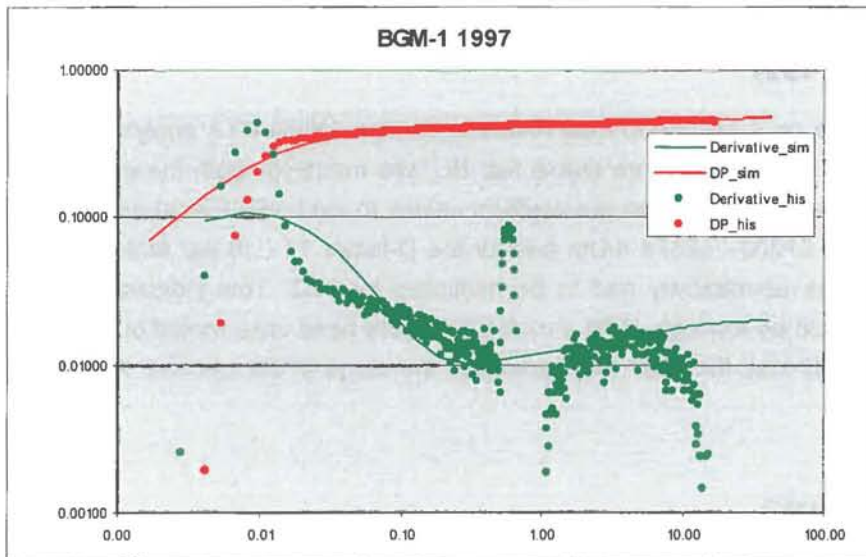


**Figure 3-8 Match of BGM-1 well test from 1997 with phase2 base case UGS model, log-log-plot.**

### 3.6 BGM-7 well test modeling results

The KH values established by well test modeling more conform to PTA analysis. The interpretation done in Phase2 has indicated that there is a significant difference between the well test-KH interpreted from the build-ups than from the drawdowns, see Figure 3-9. This difference is up to a factor 10 higher for the drawdown-KH. It is believed that this non-linear behaviour can be explained by an increase in reservoir-height during the drawdowns as the horizontal barriers below the perforations are breached by the large dP. Just below the perforations in BGM-7, relatively high-permeable layers are located. This non-linear effect can not be explained by an increase of the radius of investigation during the DD vs. the BU as the DD-time is equal to or less than the BU-time. The importance of this effect is significant as the future UGS-wells will produce at much



higher rates and drawdowns than seen during the BGM-7 well tests.

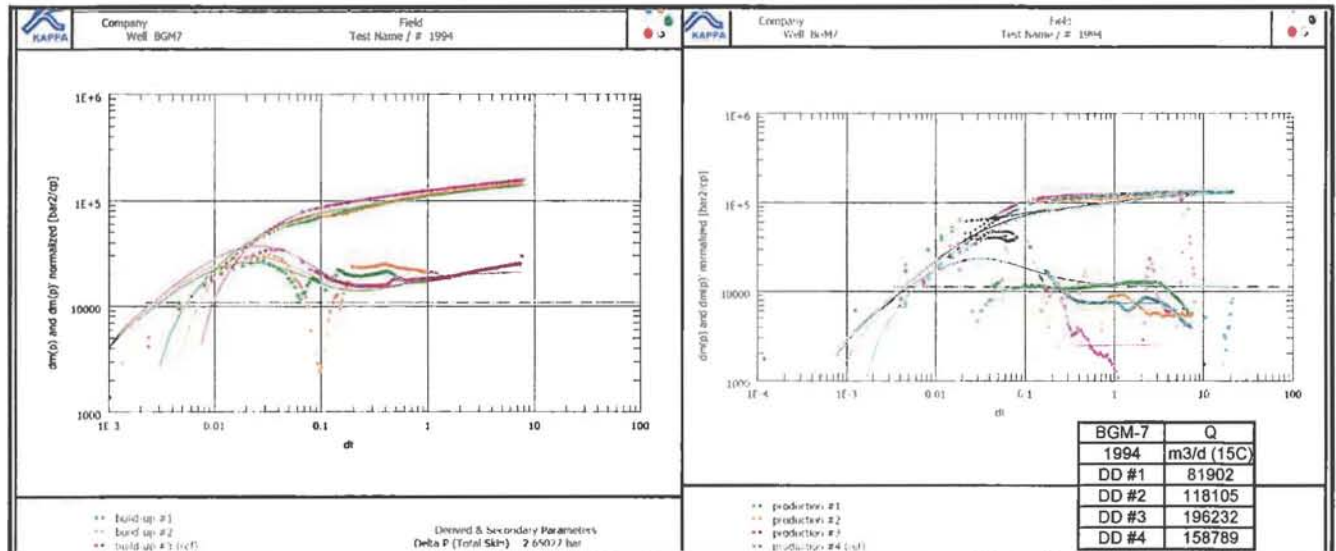


**Figure 3-9** PTA-analysis of the 1994 well test in BGM-7. Log-log plot of the BU's (left) and DD's (right). The KH from the BU's is 200-277 mDm, from the DD's a KH is calculated of 700 to over 2000 mDm for DD#1, resp. DD#3.

### 3.6.1 BGM-7 well test 1994

The isochronal well test in BGM-7 of 1994 was done with 4 different offtake-rates. The BU and DD-plots are displayed in Figure 3-9. In Eclipse the last BU was modeled as this had suffered least from liquid drop-out problems. The KH-results for the BU are similar to the KH found earlier with PTA-analysis. In Figure 3-10, the BU-periods match very well, while the DD's are much too high. The non-Darcy skin value found by PTA analysis of ca  $17 / [\text{MMm}^3/\text{d}]^{-1}$  could however not be confirmed with the low flow-rates and only 3 DD's available. Results from matching BU#3 with the base case BAG25\_ALT5\_DISMIDHIGHKV\_BELL050 model are:

- KH = 194 mDm (BU#3)
- Perf-height = 8.4 m
- K = 23 mD (Hres 8.4 m)
- Kz = 0 mD below perfs
- $D (dS/dQ) = 0 / [\text{MMm}^3/\text{d}]^{-1}$

Without the horizontal barrier, the log-log plot of BU#3 did not match up, see Figure 3-11. The DD's were matched with the same parameters as above, albeit with a multiplier of 3 on permeability, see Figure 3-10. It can clearly be seen that the BU's are now too quick compared with historical data.

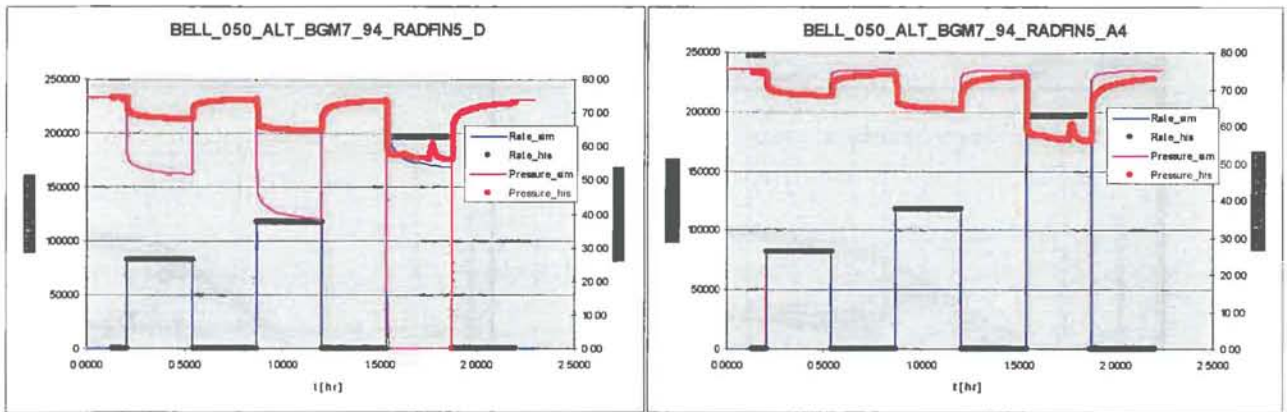


**Figure 3-10 Match of BGM-7 well test from 1994 with phase2 base case UGS model, left BU-match, right DD-match.**

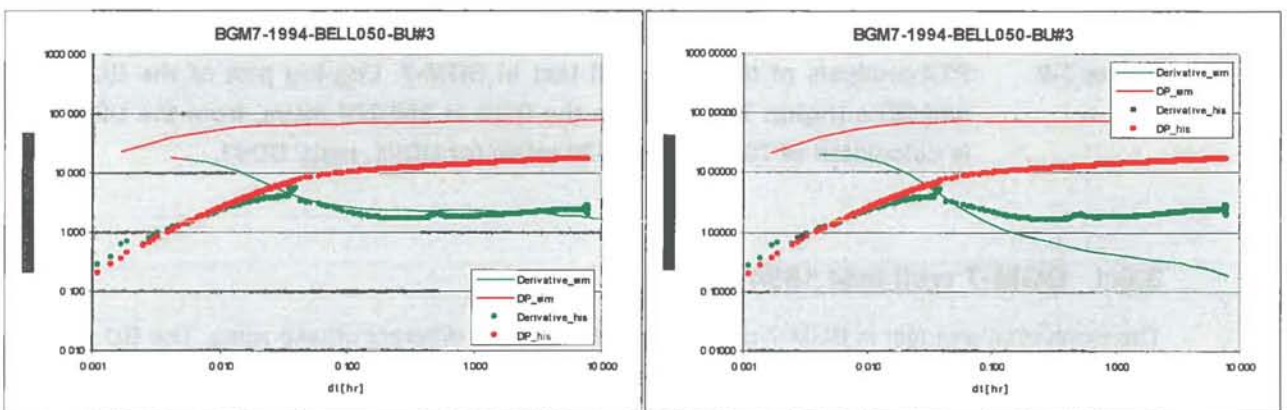


**Figure 3-11 Match of BGM-7 well test from 1994 with phase 2 base case UGS model, log-log-plot of BU#3 with horizontal barriers below perfs (left) and without  $K_z=0$  below perfs (right).**

### 3.6.2 BGM-7 well test 1997

The 1997 well test basically confirmed the results found by the 1994 test. The BELL050 model was taken for modeling, the horizontal barrier included below the perfs. The resulting KH-value for the last BU was a bit higher than previously found; this was also the case with PTA-analysis (Eclipse 194 / 232 mDm vs. PTA 308 / 330 mDm). The DD's were matched with a KH of 1060 mDm (RADFIN5\_E) and no non-Darcy skin, a factor 5 higher than the BU-value. In hindsight, the permeability-value could also have been increased and a non-Darcy skin introduced, but with only two DD's and BU's this is difficult to constrain. The BU-match results are thus:

- KH = 232 mDm (BU#1) (BELL\_050)
- Perf-height = 17 m
- K = 14 mD (Hres 17 m)
- $K_z = 0$  mD below perfs
- $D (dS/dQ) = 0 / [MMm^3/d]^{-1}$

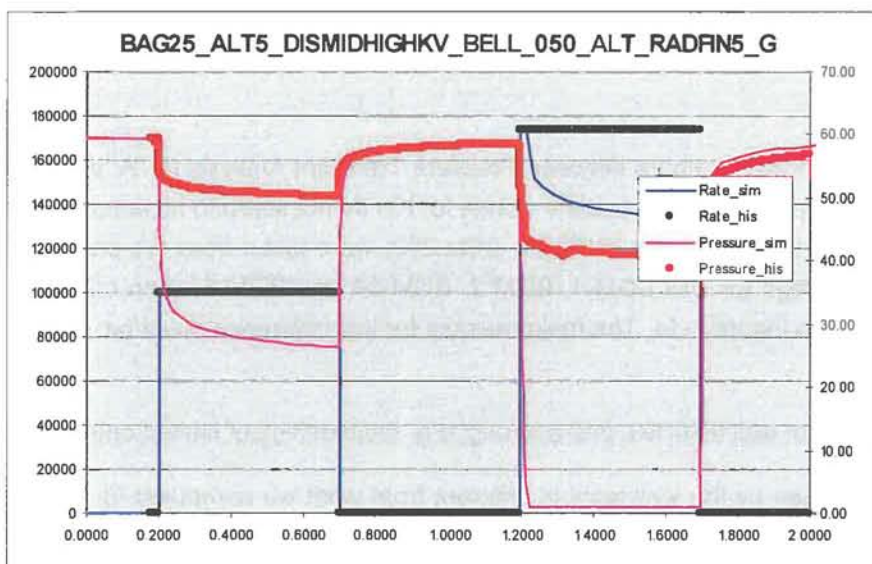


**Figure 3-12 Match of BGM-7 well test from 1997 with phase 2 base case UGS model, rate (left) and pressure (right) vs. time (hours). Note that while BU#1 matches well, the drawdowns are much too large.**

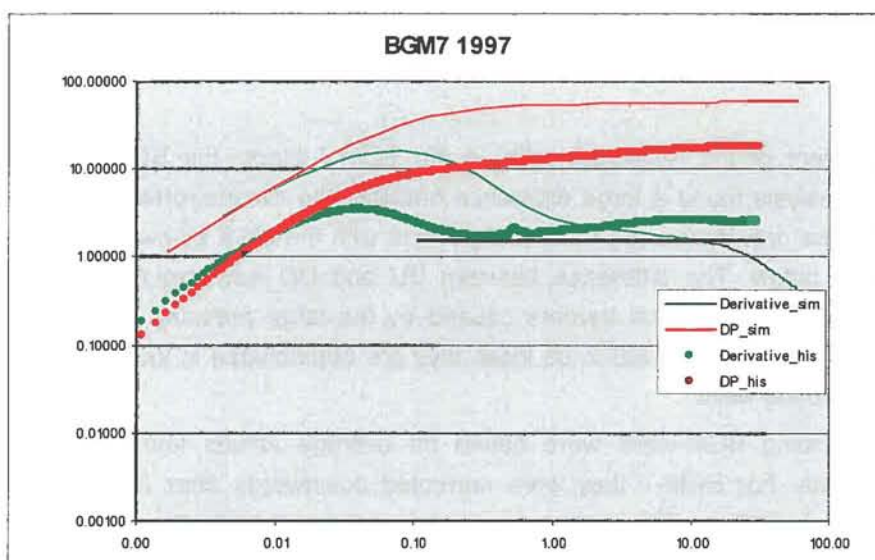


**Figure 3-13 Match of BGM-7 well test from 1997 with phase 2 base case UGS model, log-log-plot. The near wellbore region did not match perfectly, the KH is approximately correct.**

### 3.7 Conclusion

The permeability (KH) in the base case model, which is used for the future UGS well-productivity, is in the correct range for the modeled well tests of BGM-1. With the perforation-intervals taken from the history files, the permeability multipliers needed for the correct drawdowns were between 0.5 and 1.5. For the BGM-7 well test, the results are more ambiguous. The BU's did not need a multiplier at all to acquire the correct drawdowns, which suggest the model is OK here. For the BGM-7 drawdowns however, the permeability needed to be multiplied with a factor 3 to 5, without

implementing non-Darcy skin. The needed KH could also be achieved with a larger perforated reservoir section open to flow.

Although the well test values for KH compare between Pressure Transient Analysis (PTA, phase 2) and well test modeling (WTM, phase 4), the absolute values for KH do not seem to fit perfectly, see Table 3-4. The KH values for the base case (INTERA\_BELL050) were taken from the perforated zones only. Still they are too high for well BGM-1, BGM-2, BGM-3A and BGM-8 when compared with the KH from PTA, see also Figure 3-14. The main reasons for this difference could be:

1. The Eclipse modeling of well tests like this is wrong, e.g. the handling of limited entry wells.
2. The 'K' average as seen by the well tests is different from what we computed for Eclipse (arithmetic).
3. The 'H' we compute from the perforated zone in Eclipse is too high, i.e. in reality the well does not see the whole perforated zone-height.
4. The wells could also have sustained some damage in the course of production life, making the well test values unrepresentative or were placed in degraded fault zone with less permeability than in the model (BGM-2).

With respect to the placement of the horizontal wells in the BGM-7 block, the BGM-7 KH is especially important. PTA analysis found a large difference between the KH interpreted from the BU and from the DD's. As the drawdowns are more comparable with the UGS operations, these are mentioned in the table below. The difference between BU and DD was explained by the breaching of thin, low-permeable, horizontal barriers caused by the large pressure differentials during the DD. As these barriers are expected to be local, they are not included in the model and less important for future horizontal wells.

The skin-values for the existing BGM-wells were based on average values found by PTA-interpretation of the well-tests. For BGM-7 they were corrected downwards after the well test modeling interpretation done in Eclipse. The used values are  $S = 0$  for all wells. Non-Darcy skin value  $D = 20 \text{ [MMsm}^3/\text{d}]^{-1}$  for BGM-1 and BGM-5,  $D = 10$  for BGM-2, BGM-6A and BGM-8A and  $D = 0$  for BGM-7, see Table 2.5 of the Phase 2 report [1].

An overview of the welltest modeling runs is given in Appendix I.

Well	Date	Perf. Length	KH perforated - Eclipse models [mDm] PHASE 4						
			KH PTA [mD* m]	KH WTM [mD* m]	InterA_bell050	InterB_bell033	InterA_bell080	HighP	InterA_Ubell050
BGM1	1997	116.5	57300	20000-50000	86034	56735	119729	200880	81381
BGM2*	1996	95	13110		20099	13256	32158	45663	22215
BGM3A	1990	22	992		8141	2340	13025	9481	1879
BGM5*	1994	50	66150		45336	30173	72538	93774	46339
BGM6	2007	62	22400		18309	8985	29963	28255	15424
BGM7	1997	17	2000	600-1000	202	135	324	1125	548
BGM8*	1999	50	27462		55303	36540	88485	144044	68469

**Table 3-4 Comparison of KH values as found by PTA-analysis of the build-up period (with Kappa, see phase 2), by well test modeling with Eclipse100 and as found for the existing BGM wells in the phase4 models. For BGM-7 the KH of the drawdowns is compared. The KH in the models is taken from the perforated sections at the time of the test. The (\*) behind some of the wells indicates that the KH values for PTA analysis come from interpretation done by TAQA.**

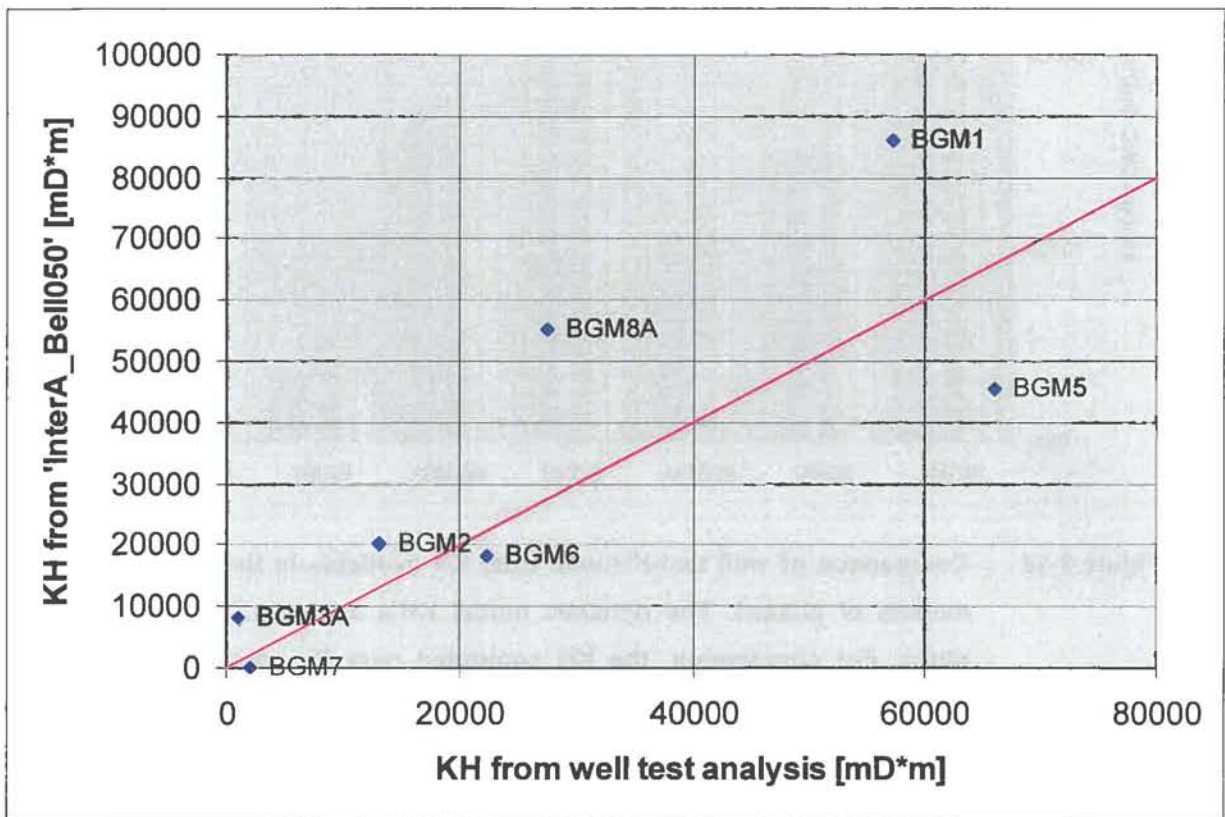


**Figure 3-14 Comparison of KH values as found by PTA-analysis, well test modeling with Eclipse100 and as found for all existing BGM wells in the Phase4 models (Table 3-4). The line plotted is  $y=x$ .**

Well	Date	Perf. Length	KH Reservoir Section - ECLIPSE MODELS PHASE 4						
			KH PTA [mD* m]	KH WTM [mD* m]	InterA_bell050	InterB_bell033	InterA_bell080	HighP	InterA_Ubell050
BGM1	1997	116.5	57300	20000-50000	122085	81390	195336	118467	122621
BGM2*	1996	95	13110		31210	20807	49936	30887	31018
BGM3A	1990	22	992		16925	11283	27080	11348	8775
BGM5*	1994	50	66150		91767	61178	146828	90779	87993
BGM6	2007	62	22400		63057	42038	100892	34591	57273
BGM7	1997	17	2000	600-1000	2261	1507	3618	1777	2157
BGM8*	1999	50	27462		168102	112068	268963	163725	167175

**Table 3-5** As Table 3-4, but now KH values from PTA and WTM compared with total reservoir KH in the phase4 models.

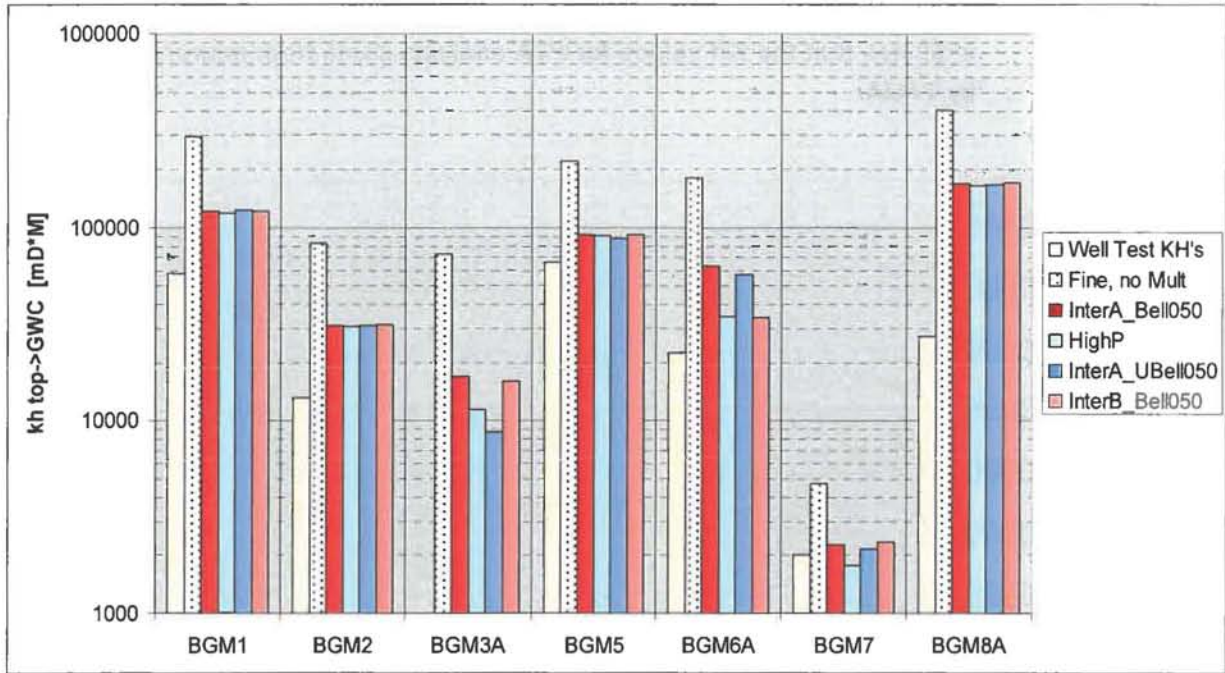


**Figure 3-15** Comparison of well test-KH with total KH available in the various dynamic models of phase4. The dynamic model KH's are over the full top→GWC range. For comparison, the KH computed over the static model, without upscaling or multiplier (BELL or otherwise) is also shown ('Fine'). For the BELL033 and BELL080 models, the KH-values are 2/3 and 8/5 of BELL050. Note that both well BGM3A and BGM6A are not used in property modeling [1], hence there is more scatter between the dynamic models for these wells.